

# Assessment of the impacts of cloud chemistry on surface SO<sub>2</sub> and sulfate levels in typical regions of China

Jiayan Lu<sup>1</sup>, Sunling Gong<sup>1,5\*</sup>, Jian Zhang<sup>1</sup>, Jianmin Chen<sup>2,3,4</sup>, Lei Zhang<sup>1</sup>, Chunhong Zhou<sup>1\*</sup>

<sup>1</sup> State Key Laboratory of Severe Weather, Key Laboratory of Atmospheric Chemistry of CMA, Institute  
of Atmospheric Composition, Chinese Academy of Meteorological Sciences, Beijing 100081, China

<sup>2</sup> Shanghai Key Laboratory of Atmospheric Particle Pollution and Prevention (LAP3), Department of  
Environmental Science and Engineering, Fudan Tyndall Centre, Institute of Atmospheric Sciences,  
Fudan University, Shanghai, China

<sup>3</sup> Center for Excellence in Urban Atmospheric Environment, Institute of Urban Environment, Chinese  
Academy of Science, Xiamen, China

<sup>4</sup> Shanghai Institute of Eco-Chongming (SIEC), No.3663 Northern Zhongshan Road, Shanghai 200062,  
China

<sup>5</sup> National Observation and Research Station of Coastal Ecological Environments in Macao, Macao  
Environmental Research Institute, Macau University of Science and Technology, Macao SAR 999078,  
China

\* Corresponding authors.

*E-mail addresses:* [gongsl@cma.gov.cn](mailto:gongsl@cma.gov.cn) (S. Gong), [zhouch@cma.gov.cn](mailto:zhouch@cma.gov.cn) (C. Zhou)

## Abstract

A regional online chemical weather model WRF/ CUACE (China Meteorological Administration  
Unified Atmospheric Chemistry Environment) is used to assess the contributions of cloud chemistry to  
the SO<sub>2</sub> and sulfate levels in typical regions of China. By comparing with several time series of in-situ  
cloud chemical observations on Mountain Tai in Shandong Province of China, the CUACE cloud  
chemistry scheme is found to reasonably reproduce the observed cloud consumption of H<sub>2</sub>O<sub>2</sub>, O<sub>3</sub> and  
SO<sub>2</sub> and the production of sulfate, and consequently is used in the regional assessment for a heavy  
pollution episode and monthly average in December 2016. During the cloudy period in a heavy pollution  
episode, the sulfate production was increased by 60-95% and SO<sub>2</sub> was reduced by over 80%. The cloud  
chemistry mainly affects the middle and lower troposphere below 5 km as well as within the boundary

layer, and contributes significantly to the SO<sub>2</sub> reduction and sulfate production in east-central China. Among the four typical regions in China, the Sichuan Basin (SCB) is mostly affected by the cloud chemistry, with the average SO<sub>2</sub> abatement about 1.0-15.0 ppb and sulfate increase about 10.0-70.0 μg/m<sup>3</sup>, followed by Yangtze River Delta (YRD) and southeast of North China Plain (NCP), where SO<sub>2</sub> abatement is about 1.0-3.0 ppb and sulfate increase is about 10.0-30.0 μg/m<sup>3</sup>. However, the cloud chemistry contributions to the Pearl River Delta (PRD) and northwest of NCP are not significant due to lighter pollution and less water vapor than other two regions. This study provides a way to analyze the over-estimate phenomenon of SO<sub>2</sub> in many chemical transport models.

Keywords: SO<sub>2</sub>, sulfate, cloud chemistry, WRF/CUACE

## 1 Introduction

Aerosols interact with radiation and clouds, directly or indirectly affecting the atmospheric radiation balance and precipitation, which in turn affects weather and climate (Twomey et al., 1984; Twomey, 1991; Charlson et al., 1992; Ramanathan et al., 2001; Pye et al., 2020). Moreover, large amounts of aerosols dispersed in the atmosphere can reduce visibility and deteriorate air quality (Molina, 2002), which is harmful to human health and ecosystem (Xie et al., 2019; Sielski et al., 2021).

In addition to direct emissions, aerosols are mostly produced secondarily through the oxidation of precursor gases, and one of the important processes is the transformation in clouds. Global cloud coverage of about 21% to 95% provides an adequate environment for cloud chemistry processes (Kotarba, 2020; Ravishankara, 1997). As about 90% of the clouds formed in the atmosphere evaporate without deposition or forming the precipitation, large fractions of aerosols formed in them can then re-enter the atmosphere (Caffrey et al., 2001; Harris et al., 2013; Lelieveld et al., 1992). Globally, sulfate production from SO<sub>2</sub> oxidation accounts for about 80% of total sulfate, and more than half of it is produced in clouds (Hung et al., 2018; Faloon et al., 2010; Guo et al., 2012). Ge et al. (2021) found that cloud chemistry processes reduced the SO<sub>2</sub> concentrations by 0-50% in most of east-central China in all seasons. Li (2011) found that the average SO<sub>4</sub><sup>2-</sup> concentration in cloud water accounted for 53.8% of the total aerosol concentration at a Mount site. Li et al. (2020) also found that cloud processes effectively

reduced atmospheric O<sub>3</sub> and SO<sub>2</sub> concentrations by an average of 19.7% and 71.2%, respectively, at  
55 Mount Tai.

Multiphase oxidation of SO<sub>2</sub> in aerosol particles in high humidity environment is one of the main causes of explosive growth of particulate matter in East Asia haze (Guo et al., 2014; Cheng et al., 2016; Song et al., 2019). From observations and laboratory works, four main pathways were found for this kind of oxidation of SO<sub>2</sub>, i.e. by H<sub>2</sub>O<sub>2</sub>, O<sub>3</sub>, NO<sub>2</sub>, and transition metal ions (TMIs) (Iibusuki and  
60 Takeuchi, 1987; Martin et al., 1991; Alexander et al., 2009; Harris et al., 2013; Cheng et al., 2016; Wang et al., 2016). Additional pathways of organic peroxides (ROOH) (Yao et al., 2019; Wang et al., 2019; Ye et al., 2018; Dovrou et al., 2019), photolysis products of nitrate (pNO<sub>3</sub><sup>-</sup>) (Gen et al., 2019a; 2019b), and excited triplet states of photosensitizer molecules (T\*) (Wang et al., 2020) have also been found recently to be important for multiphase oxidation of SO<sub>2</sub> during very heavy hazy days. Unfortunately there are  
65 still much uncertainties and gaps to put all of those pathways into model applications from observational and laboratory studies (Pye et al., 2020; Ravishankara, 1997; Liu et al., 2021). Several regional and global models have tried to include only two, O<sub>3</sub> and H<sub>2</sub>O<sub>2</sub>, in-cloud oxidant in cloud chemistry mechanisms (Park et al., 2003; Tie et al., 2005; Salzen et al., 2000; Chapman et al., 2009; Leighton and Ivanova, 2008; Ivanova and Leighton, 2008). A very few models can simulate the pathway of NO<sub>2</sub>,  
70 TMIs of Fe or Mn ions (Ge et al., 2021; Binkowski and Roselle, 2003; Chang et al., 1987; Terrenoire et al., 2015; Meleux, et al., 2013).

There has been very serious air pollution in central-east China where four heavy pollution regions of North China Plain (NCP), Yangtze River Delta (YRD), Sichuan Basin (SCB) and Pearl River Delta (PRD) are located (Yao et al., 2021; Zhang et al., 2012). Although many global and regional models  
75 have contained sulfate formation mechanisms by cloud chemistry, few models have assessed its contribution, especially the lack of detailed assessment of regional cloud chemistry on sulfate and SO<sub>2</sub> in China. Regional chemical models have reported the over-estimate of SO<sub>2</sub> (Buchard et al., 2014; He et al., 2015; Wei et al., 2019; Sha et al., 2019; Georgiou et al., 2018). The inadequate inclusion or lack of cloud chemistry of SO<sub>2</sub> consumption simulations is one of the main causes (Ge et al., 2021). Therefore, it is  
80 very important and necessary to quantify the contribution of cloud chemistry in these typical regions in

central-east China and get a better understand of multi-dimensional pollution interactions, especially between the upper layer and the surface.

This study is intended to use an on-line coupled chemical weather platform of WRF/CUACE, to analyze and evaluate the SO<sub>2</sub> in-cloud oxidation process in the four polluted regions in China, with two objectives: (1) evaluating the cloud chemistry scheme in WRF/CUACE by the in-situ cloud chemistry observations at Mount Tai in summers of 2015 and 2018; and (2) quantifying the contributions of cloud chemistry to the SO<sub>2</sub> and sulfate changes in a typical winter pollution month of December 2016 with a very long lasting heavy pollution episode. It is aimed to establish a system to assess the relative contribution of cloud chemistry to SO<sub>2</sub> oxidation and sulfate productions vs. other clear-sky processes.

## 2 Model description and Methodology

### 2.1 Cloud chemistry in WRF/CUACE

WRF/CUACE is an on-line coupled chemical weather model under the WRF frame work with a comprehensive chemical module - CUACE, which is developed at CMA (China Meteorological Administration) with a sectional aerosol physics, gas chemistry, aerosol-cloud interactions and thermodynamic equilibrium (Zhou et al., 2012; Zhou et al., 2016; Gong et al., 2003; Gong and Zhang, 2008; Zhang et al., 2021), with seven types of aerosols, i.e. black carbon, organic carbon, sulfate, nitrate, ammonium, soil dust, and sea salt, and more than 60 gaseous species. The aerosol size spectrum is divided into 12 bins with fixed boundaries of 0.005-0.01, 0.01-0.02, 0.02-0.04, 0.04-0.08, 0.08-0.16, 0.16-0.32, 0.32-0.64, 0.64-1.28, 1.28-2.56, 2.56-5.12, 5.12-10.24 and 10.24-20.48  $\mu\text{m}$ . The system can simulate the concentrations of PM<sub>10</sub>, PM<sub>2.5</sub> and O<sub>3</sub> as well as visibility. A complete heterogeneous chemistry module has been built in CUACE for nine gas-to-particle heterogeneous reactions including SO<sub>2</sub> to sulfate (Zhou et al., 2021, Zhang et al., 2021). The cloud chemistry mechanism in CUACE considers the pathways of multiphase oxidation of SO<sub>2</sub> by H<sub>2</sub>O<sub>2</sub> and O<sub>3</sub> in both stratocumulus and convective clouds (Gong et al., 2003; Von Salzen et al., 2000). The transport and chemical effects of sulfur in convective clouds are calculated based on a convective cloud model by WRF. Within the cloudy part of a grid box, the first-order rate constant (in s<sup>-1</sup>) of S(IV) oxidation is given by the

following expression:

$$F = \left| \frac{1}{C_{S(IV)}} \frac{dC_{S(IV)}}{dt} \right| = F_1 C_{O_3} + F_2 C_{H_2O_2} \quad (1)$$

where  $C_{S(IV)}$  is the total concentration of S(IV) (gas phase plus dissolved),  $C_{O_3}$  is the total concentration  
 110 of  $O_3$ , and  $C_{H_2O_2}$  is the total concentration of hydrogen peroxide.

The effective rate constants  $F_1$  and  $F_2$  are given by the following expressions:

$$F_1 = R_{O_3} f_1 \quad (2)$$

$$F_2 = R_{H_2O_2} f_2 \quad (3)$$

The reaction rate constants  $R_{O_3}$  and  $R_{H_2O_2}$  refer to Maahs (1983) and Martin et al. (1984):

$$R_{O_3} = \left\{ 4.4 \times 10^{11} \exp(-4131/T) + 2.61 \times 10^3 \exp(-966/T) \right\} [H^+]^{-1} (Ms)^{-1} \quad (4)$$

$$R_{H_2O_2} = 8 \times 10^4 \exp[-3650(1/T - 1/298)] \left\{ 0.1 + [H^+] \right\}^{-1} (Ms)^{-1} \quad (5)$$

In Equations (2) and (3), the factors  $f_1$  and  $f_2$  represent the partitioning of the substance between  
 the aqueous and gas phases and are determined by the Henry's law coefficients.

$$f_1 = \gamma f_{SO_2} f_{O_3} K_S \bar{K}_{HO} \quad (6)$$

$$f_2 = \gamma f_{SO_2} f_{H_2O_2} \bar{K}_{HS} \bar{K}_{HP} \quad (7)$$

where  $\gamma$  is the dimensionless volume fraction of liquid water in the cloud. The parameters  $f_{SO_2}$ ,  $f_{O_3}$   
 and  $f_{H_2O_2}$  are the proportions of individual substances in the gas phase, which are calculated from the

dimensionless Henry's law constant and  $\gamma$ .

$$f_{SO_2} = (1 + \gamma \bar{K}_{HS} K_S)^{-1} \quad (8)$$

$$125 \quad f_{O_3} = (1 + \gamma \bar{K}_{HO})^{-1} \quad (9)$$

$$f_{H_2O_2} = (1 + \gamma \bar{K}_{HP})^{-1} \quad (10)$$

with

$$K_S = \bar{K}_{HS} \left( 1 + \frac{K_{1S}}{[H^+]} + \frac{K_{1S} K_{2S}}{[H^+]^2} \right) \quad (11)$$

130 The Henry's law constants used in (6) to (8) are listed in Table 1.

In order to consider the dependence of the oxidation rates on the pH, the  $H^+$  concentration is calculated from ions balance.

$$[H^+] + [NH_4^+] = [OH^-] + 2[SO_4^{2-}] + 2[SO_3^{2-}] + [HSO_3^-] + [NO_3^-] + [HCO_3^-] \quad (12)$$

135 From Eqs. (1) ~ (12), CUACE can simulate the oxidation rates of  $SO_2$  by  $H_2O_2$  and  $O_3$  mainly in the liquid and gaseous environment in both stratocumulus and convective clouds in three-dimensional way.

## 2.2 Assessment criteria

Three variables, RTCLD, DT, and RT, are defined to assess the impact of the cloud chemistry on  $SO_2$  and sulfate. RTCLD refers to the concentration change ratio of substance  $i$  before and after the cloud chemical processes in a model run.

$$140 \quad RTCLD(i) = 1 - \frac{BECLD(i)}{AFCLD(i)} \quad (13)$$

where BECLD and AFCLD denote the concentrations of component *i* before and after the cloud chemical processes, respectively, and *i* denotes the chemical component of SO<sub>2</sub>, O<sub>3</sub>, H<sub>2</sub>O<sub>2</sub>, and sulfate.

The DT indicates the difference in concentration of substance *i* with (CLD) and without (nCLD) cloud chemistry module activated.

$$145 \quad DT(i) = CLD(i) - nCLD(i) \quad (14)$$

and the RT represents the concentration ratio change of the substance *i* with and without cloud chemistry in separate model runs:

$$RT(i) = 1 - \frac{nCLD(i)}{CLD(i)} \quad (15)$$

## 2.3 Methodology

### 150 2.3.1 Model Evaluation – Case 1

Mount Tai at an altitude of about 1545 m, located in central Shandong Province, is the highest point of the North China Plain. As the Riguan Peak of Mount Tai is far from pollution sources, and the water vapor conditions favors very much cloud formations in summer, it is an ideal observation site for cloud chemistry observation (Li et al., 2017; Li et al., 2020a; Li et al., 2020b). The observed concentrations of 155 SO<sub>2</sub>, O<sub>3</sub>, H<sub>2</sub>O<sub>2</sub> and sulfate in cloudy conditions from June 19 to July 30, 2015 and from June 20 to July 30, 2018 with time interval of 1 h are obtained to evaluate the cloud chemistry scheme in WRF/CUACE (Li et al., 2017; Li et al., 2020a; Li et al., 2020b).

WRF/CUACE is set up with two-domain nesting for the evaluation, with the Riguan Peak as the central point (Fig. 1a). The horizontal resolution of outer domain (O) is 9 km with 100×104, and of the

160 inner domain (I) is 3 km with 88×94 (Fig. 1a). There are 32 vertical layers with the top pressure of 100 hPa.

### 2.3.2 Simulations of Regional Characteristics – Case 2

In order to assess the regional contribution of cloud chemistry to SO<sub>2</sub> and sulfate in CUACE, December 2016 is selected with a widespread heavy pollution episode occurred in North and East China from Dec. 16 to 21, covering NCP, YRD and SCB with the highest hourly PM<sub>2.5</sub> concentration exceeding 1100 µg/m<sup>3</sup> (Yuan and Ma, 2017). The simulation region is set up as shown in Figure 1b with two-level domain nesting. The outer domain (O) covers Central and East Asia with a horizontal resolution of 54 km and a grid of 139×112. The inner domain (I) covers most of China on the eastern side of the Qinghai-Tibet Plateau with a horizontal resolution of 18 km and a grid of 157×166. The vertical layer number of the model is the same as that in the Case 1.

Since the cloud water is the reaction pool of cloud chemistry, whether the simulation of cloud water is reasonable or not is directly related to the effectiveness of cloud chemistry. Both the cloud water and rainwater from WRF are coupled to the cloud chemistry module and main physics configurations are listed in Table 2.

## 175 2.4 Meteorological, Pollution and Satellite Data

For both cases, the meteorological initial and boundary conditions for WRF/CUACE are from NCEP (National Centers for Environmental Prediction) FNL global reanalysis at a resolution of 1°×1° with 6-h interval. The chemical lateral boundary conditions are from NOAA (National Oceanic and Atmospheric Administration) Meteorological Laboratory Regional Oxidant Model (NALROM) (Liu et al., 1996). The model is run in a restart way with a 5-day spin-up.

FY-2G cloud image data of CMA with an 1 h interval is used to evaluate the cloud in both cases. Routine observations in 3 h interval from 23 meteorological stations of CMA and hourly pollution observations from 132 stations of the China General Environmental Monitoring Station are used to evaluate the meteorological fields and pollutants for December 2016. Meteorological elements include 2



185 m temperature, 2 m relative humidity, and 10 m wind speed.

The MEIC (Multi-resolution Emission Inventory for China) inventory, at a resolution of  $0.25^\circ$ , is used as the anthropogenic emissions with the species of sulfur dioxide ( $\text{SO}_2$ ), nitrogen oxides ( $\text{NO}_x$ ), carbon monoxide ( $\text{CO}$ ), ammonia ( $\text{NH}_3$ ), black carbon ( $\text{BC}$ ), organic carbon ( $\text{OC}$ ), non-methane volatile organic compounds (NMVOCs),  $\text{PM}_{2.5}$  and  $\text{PM}_{10}$  by five sectors of power, industry, transportation, residential, and agriculture (Li et al., 2017; Zheng et al., 2018). The emission base year of 2015 and 2017 are used for Case-1, of 2016 for Case-2, respectively.

### 3 Results and Discussions

#### 3.1 Evaluation of the cloud chemistry mechanism

In order to verify the cloud chemistry mechanism in WRF/CUACE, the simulation results are compared with the observations at Mount Tai. By analyzing the satellite cloud images in and around Mount Tai and matching with the available observed data, two time periods with clouds from June 19 to July 30, 2015 and June 20 to July 30, 2018 are selected for the comparisons, defined as "cloud process-1" (CP-1) and "cloud process-2" (CP-2), respectively. The simulated results for chemical species are illustrated in scatter plots (Fig. 2), which reveals that the simulated concentrations of  $\text{SO}_2$ , sulfate,  $\text{O}_3$ , and  $\text{H}_2\text{O}_2$  are all within a factor of two of the observations when cloud chemistry occurs, indicating reasonable agreement between simulations and observations for both CP-1 and CP-2 cases. The sulfate underestimates are clear in both CP-1 and CP-2 cases, which was reported by other modeling results before as well (Tuccella et al., 2012; Huang et al., 2019; Ge et al., 2022).

The statistics of correlation coefficients (R), relative average deviation (RAD), and normalized mean deviation (NMB) between hourly simulated and observed  $\text{SO}_2$ ,  $\text{O}_3$ ,  $\text{H}_2\text{O}_2$  and sulfate are shown in Table 3. Among them, the simulated and observed averages of  $\text{SO}_2$  are very close in both CP-1 and CP-2, with the RAD about -3.4% and -6.1% and with the RAD for other species in the range of 8.7-55.0%. The R for the four species are 0.34, 0.33 and 0.78 and 0.32 for CP-1, and 0.47, 0.40, 0.06 and 0.54 for CP-2, respectively. Although the R, RAD, and NMB of  $\text{H}_2\text{O}_2$  in CP-2 is only 0.06, 18.0%, and -19.6%,

210 the simulated mean value of H<sub>2</sub>O<sub>2</sub> is closer to the observed mean value than that in CP-1 (RAD = 22.4%,  
NMB = -36.6%). For sulfate, the simulated correlations are good with R of 0.32 and 0.54 in CP-1 and  
CP-2, respectively, but the model underestimates sulfate concentrations with NMB of -71.0% and -  
59.4% in CP-1 and CP-2. This indicates that although the model is able to simulate the trend of sulfate  
concentrations, the simulated concentrations are lower than the observed values which may be due to the  
215 incompleteness of other cloud chemistry mechanisms or the bias of liquid water content in the cloud  
physics.

Another interesting point that is simulated correctly by the model is the increasing trend of H<sub>2</sub>O<sub>2</sub> and  
the decreasing trend of SO<sub>2</sub> from CP-1 to CP-2 (Table 3), representing year of 2015 and 2018,  
respectively. It was found that the observed and simulated mean values of H<sub>2</sub>O<sub>2</sub> are 26.5 and 16.8 μM in  
220 CP-1, to 46.9 and 32.4 μM in CP-2, respectively. For SO<sub>2</sub>, the observed and simulated mean values are  
2.2 and 2.3 μg/m<sup>3</sup> in CP-1, to 0.6 and 0.6 μg/m<sup>3</sup> in CP-2, respectively. The simulation results are  
consistent with the trends of other observational studies (Shen et al., 2012; Li et al., 2020b; Ren et al.,  
2009; Ye et al., 2021) The SO<sub>2</sub> trends may be attributed to the relevant national emission control  
measures, but the increasing trend of H<sub>2</sub>O<sub>2</sub> and O<sub>3</sub>, indicating an increasing oxidation ability of the  
225 atmosphere in the eastern part of China, needs further investigations.

To further evaluate the model performance, Figure 3 shows the satellite cloud maps, simulated  
column clouds, and simulated liquid water content at 8:00 LST on June 24, and 8:00 LST on June 25 in  
CP-1. At both times, the model's column clouds and liquid water distribution are consistent with the  
cloud distribution observed by the satellites. This indicates that the model's simulation of cloud  
230 distribution regions is realistic and the cloud chemistry initiation mechanism, cloud-water environment,  
is reasonably simulated.

Figure 4 shows the RTCLD of SO<sub>2</sub> and simulated liquid water contents at 2:00 and 8:00 LST on  
June 24, and 2:00 and 8:00 LST on June 25 in CP-1 at the Taishan's observation site. The results  
indicate that the RTCLD of SO<sub>2</sub> distribution simulated during these periods is consistent with the cloud  
235 liquid water, with a SO<sub>2</sub> RTCLD reduction of more than 80% within the cloud region of Mount Tai and  
most of Shandong province, which is consistent with the cloud chemistry observation studies by Li

(2020).

In summary, the cloud chemistry mechanism in WRF/CUACE is reasonable to reproduce the cloud chemistry for the gaseous pollutant SO<sub>2</sub>, sulfate and the important oxidants of O<sub>3</sub> and H<sub>2</sub>O<sub>2</sub> in a cloud environment. The simulations are within a factor of two of the observations, the bias is small, and the cloud chemistry occurs in agreement with the model cloud distribution. In addition, CUACE is also able to simulate the SO<sub>2</sub> decreasing trend and O<sub>3</sub> and H<sub>2</sub>O<sub>2</sub> increasing trends with year.

### 3.2 Assessment of the impacts of cloud chemistry on regional SO<sub>2</sub> and sulfate

This session will further assess the contribution of cloud chemistry for the four main pollution regions of NCP, YRD, PRD, and SCB (Fig. 1) in China for the whole December of 2016 (as DEC thereafter) and a heavy pollution episode (as HPE thereafter) occurred during month (Dec. 16-22) as selected for Case 2.

#### 3.2.1 Meteorological evaluation

As the driving force of air pollution and cloud chemistry, the simulated results of 2 m temperature (T2), 2 m relative humidity (RH2) and 10 m wind speed (WS10) in DEC and HPE are shown in Table 4. The correlations between simulated and observed values of all three meteorological elements are very close both in DEC and HPE for the four regions, indicating a good model performance. The temperature correlation is the best in DEC, followed by humidity and then wind speed, which is consistent with previous researches (Zhou et al., 2012; Wang et al., 2015; Gao et al., 2016). The RMSE of wind speeds all range from 1.03 to 1.50 m/s, falling within the criteria (less than 2 m/s) to define “good” model performance in stagnant weather proposed by Emery et al. (2001). The RSME of wind speed for HPE is smaller than that for DEC, which indicates that the model can well capture the static wind even though it is very small.

Figure 5 shows the satellite cloud image, simulated column cloud and simulated liquid water content for the maturation and dissipation stages (19-22 Dec.) of the HPE. The satellite image shows that the cloud coverage region is mainly in the southwest including SCB on the 19<sup>th</sup>, covering most of

eastern China including NCP, YRD, PRD and SCB on the 20<sup>th</sup> and the 21<sup>st</sup>, and then moving eastward outside of China on the 22<sup>nd</sup> (Fig. 4 a1-d1). The simulated clouds fit well with the satellite images (Fig. 4 a2-d2). Since the cloud chemistry occurs in the cloud area, the cloud chemistry mainly affects NCP, YRD and SCB regions as PRD has relatively much less cloud. The column liquid water distribution also moves from west to east as the episode developed (Fig. 5 a3-d3), but is located more southern part of eastern China than that of the clouds. In SCB and YRD, the liquid water content is more abundant, reaching over 100.0 g/m<sup>2</sup>, than that in PRD, only up to 10.0 g/m<sup>2</sup>. NCP has the least liquid water content of about 0.001-100.0 g/m<sup>2</sup> among the four regions, especially in Beijing, Tianjin and Hebei Province less than 10.0 g/m<sup>2</sup>, mostly due to the dry environment and partly due to the overestimated temperature and underestimated humidity in Table 4.

The above analysis shows that the model basically reproduces the meteorological field in December and heavy pollution periods, which provides a reasonable meteorological background basis for the effective simulation of pollution as well as cloud chemistry.

### 3.2.2 Pollutants Evaluation

The simulated hourly PM<sub>2.5</sub>, O<sub>3</sub> and SO<sub>2</sub> concentrations in four regions are compared with the observations (Table 5). The simulations are all within a factor of two of the observations (figure omitted), and the mean values of the three pollutants simulated in the four regions are very close to the observations, indicating that model captures well the variability of PM<sub>2.5</sub>, O<sub>3</sub> and SO<sub>2</sub> concentrations for both DEC and HPE. Specifically, O<sub>3</sub> correlates well with observations in all four regions for the DEC, but less satisfactory during HPE for YRD and SCB regions. For PM<sub>2.5</sub>, the correlation is high for HPE in PRD with R of 0.84, and with R of 0.39 for DEC. The correlation is high for DEC in NCP, with R of 0.62, and with R of 0.30 for HPE. The correlation is high for DEC and HPE in YRD, with R of 0.73 and 0.70. The difference in correlation between DEC and HPE is small in YRD and SCB. For SO<sub>2</sub>, the model simulations are better for HPE in the three regions of NCP, YRD and SCB, than that for DEC. The R during the HPE and the DEC are 0.60 and 0.48 in NCP, 0.61 and 0.45 in YRD, and 0.49 and 0.19 in SCB, respectively. The correlations between observations and simulations for HPE and DEC in PRD are not significantly different, with R of 0.32 and 0.39, respectively. Therefore, the following part of this

paper will focus on assessing the effects of cloud chemical processes.

### 3.2.3 Assessment of regional contributions

The regional impacts of cloud chemical processes on surface SO<sub>2</sub> and sulfate are analyzed for DEC and for HPE. The pollution episode (HPE) is investigated with respect to the developing stage HPE-1 (Dec. 16-18), the maturity stage HPE-2 (Dec. 19-21) and to the dissipation stage HPE-3 (Dec. 22) for the four pollution regions of NCP, YRD, PRD and SCB.

The average impact of cloud chemistry on surface SO<sub>2</sub> and sulfate for DEC (Fig. 6, DT(SO<sub>2</sub>) and DT (sulfate)) is assessed. It is found that SO<sub>2</sub> declination for DEC is concentrated mostly in the central-eastern part of China, by an average of 0.1-1.0 ppb in most regions by cloud chemistry. SO<sub>2</sub> concentrations are reduced by 0.5-3.0 ppb in most part of NCP, YRD, PRD and SCB regions. Among them, there is a relatively strong center by declining 3.0-10.0 ppb in SCB. Correspondingly, sulfate growth is mainly centering in SCB, with the increased maximum center up to 20.0-50.0 µg/m<sup>3</sup>. Sulfate concentrations are increased by 10.0-20.0 µg/m<sup>3</sup> in most part of NCP, YRD and PRD, and increased 5-10.0 µg/m<sup>3</sup> in others.

The spatial distribution of cloud chemistry contribution to SO<sub>2</sub> and sulfate during HPE-2 is analyzed (Fig. 7, DT(SO<sub>2</sub>) and DT(sulfate)) on the HPE-2. It is shown that the SO<sub>2</sub> concentration decreases most significantly in SCB, exceeding 1.0-3.0 ppb in most region, to 3.0-10.0 ppb in the central region. In YRD, PRD and NCP, the reduction reaches 1.0-3.0 ppb in most region while the smallest decrease is below 1.0 ppb in the northern part of NCP. Meanwhile, in terms of regional distribution, the regions of increasing sulfate and decreasing SO<sub>2</sub> concentrations are correlated, but not identical. Sulfate concentration increases by more than 10.0 µg/m<sup>3</sup> from the southern part of NCP to central China and from most of the eastern part of SCB to the YRD region. Sulfate concentration increases by more than 20.0 µg/m<sup>3</sup> in SCB and up to more than 50.0 µg/m<sup>3</sup> in the central region of SCB, by 20.0-30.0 µg/m<sup>3</sup> in the central region of YRD, and by 5.0-20.0 µg/m<sup>3</sup> in the whole PRD region. The sulfate concentration increases up to 10.0 µg/m<sup>3</sup> in the south of NCP and along the Yangtze River from the east of SCB to the west of YRD.

315 In summary, comparing the contribution of cloud chemistry in DEC with HPE-2, it is found that the cloud chemistry in heavy pollution weather for SO<sub>2</sub> depletion and sulfate increase is mainly concentrated in the central-eastern part of China, and the four major pollution regions are also more obvious. However, SO<sub>2</sub> consumption and sulfate increase are not consistent, which is not only influenced by the local SO<sub>2</sub> concentration, but also by the cloud amount. Therefore, for SCB, where  
320 there is less polluted and has much more clouds than that in NCP, the impact of cloud chemistry on sulfate and its precursor SO<sub>2</sub> is always the most significant, for both HPE and DEC.

Exploring details into the HPE, three moments, 21:00 and 17:00 on the 20<sup>th</sup> and 21<sup>st</sup> of the HPE-2, and 12:00 on the 22<sup>nd</sup> of the HPE-3, are used to specifically analyze the contribution of cloud chemistry. It is found that the cloud chemistry influence is mainly on SCB and YRD at 21:00 LST on Dec. 20. The  
325 sulfate concentration increases (DT(sulfate)) by about 20.0-100.0 μg/m<sup>3</sup> in most parts of SCB, and the highest is about 150.0-225.0 μg/m<sup>3</sup> in its southwest (Fig. 8a). The increase is about 10.0-40.0 μg/m<sup>3</sup> in most parts of YRD, and the highest increase can reach 40-100 μg/m<sup>3</sup> in the southeast near Hangzhou Bay. At 21<sup>st</sup> 17:00 LST, it is shown that the pollution episode has moved eastward and the cloud chemistry process has a stronger impact on NCP than at the previous time (Fig. 8b). The increase center  
330 is located in Shandong Province, with up to 100.0-225.0 μg/m<sup>3</sup>, and with about 10.0-60.0 μg/m<sup>3</sup> in most of NCP. In PRD, the impact of the cloud chemistry is the least, with sulfate concentration increase of 10.0-40.0 μg/m<sup>3</sup>. At 22<sup>nd</sup> 12 LST. Although the episode has gradually dissipated, the impact still exist, with sulfate increase about 10.0-40.0 μg/m<sup>3</sup> in most of these four regions (Fig. 8c).

Above all, the contribution of cloud chemistry to surface sulfate during this HPE is the highest in  
335 the SCB, followed by the NCP, YRD and PRD, with maximum concentration increases of 225.0 μg/m<sup>3</sup>, 200.0 μg/m<sup>3</sup>, and 100.0 μg/m<sup>3</sup>, 40.0 μg/m<sup>3</sup>, respectively, and an increase of 1.0-40.0 μg/m<sup>3</sup> in other areas of the four regions. Of particular note is the North China region, where the contribution of cloud chemistry is not significant on a monthly average but is very significant and exceeds that of the YRD region at certain moments during HPE. This also provides an explanation for the explosive increase in  
340 particulate matter concentrations during HPE in this region.

Further analysis of the simulation characteristics with and without cloud chemistry on all the

regions during the HPE-2 stage (Fig. 9) and the DEC (Fig. 10), is carried out. Compared with nCLD, R of SO<sub>2</sub> in CLD increases by 0.60, 0.14, and 0.10 in YRD, SCB, and NCP, respectively, and the overestimation in NCP and PRD has been corrected during HPE-2. R also increases by 0.10, 0.03 and 0.04 in YRD, SCB and NCP for the DEC, respectively. It is obvious that the model simulates SO<sub>2</sub> concentrations better at NCP during HPE-2 than for DEC with cloud chemistry.

For PM<sub>2.5</sub>, the statistical results of the simulated mean, R and NMB in CLD and nCLD in the four polluted regions do not differ significantly between HPE-2 and DEC, but there is a significant improvement in the underestimate in NCP and SCB. Under cloud chemistry, the deviation in the NCP increases from -45.7% to -35.7% for DEC and from -52.6% to -48.2% for HPE-2. The deviation in SCB increases from -44.2% to -29.1% for DEC and from -46.5% to -32.9% for HPE-2. A significant reduction in the model's PM<sub>2.5</sub> concentration simulation bias after considering cloud chemistry, and an improvement in the underestimation at NCP and SCB has been achieved.

Moreover, the statistical results of all stations (SUM in Fig. 11) show that after considering cloud chemical simulation (CLD), the NMB of SO<sub>2</sub> decreased from 39.3% to 13.8% and the NMB of sulfate increased from -40.6% to -31.6% during the HPE-2 after the addition of cloud chemistry simulation, decreasing the simulation bias of both SO<sub>2</sub> and sulfate. This indicates that the addition of cloud chemistry to the model improves the model for SO<sub>2</sub> and sulfate simulations. The improvement of sulfate simulation in the presence of clouds also contributes to the improvement of the simulation accuracy of PM<sub>2.5</sub> mentioned above.

### 3.3 Site evaluation of cloud chemistry

Representative sites of Beijing, Nanjing, Guangzhou and Chengdu at NCP, YRD, PRD and SCB are selected to quantify the impact of cloud chemistry during the HPE. The net depletion ratio of SO<sub>2</sub> column concentration (RT(SO<sub>2</sub>)) during cloud chemistry is shown in Figure 12. It is found that SO<sub>2</sub> column concentration reduction maintained mostly a high value of over 60%, even to 80% sometimes, in Chengdu during HPE-2. In Nanjing, the SO<sub>2</sub> level is reduced by about 20-50% from 17<sup>th</sup> to 19<sup>th</sup> and up to 80% from 20<sup>th</sup> to 21<sup>st</sup> when the episode matures there. The changes of SO<sub>2</sub> in these two cities are

consistent with the changes in cloud and liquid cloud water content distributions during the HPE-2 in Figure 3. The SO<sub>2</sub> reduction in Beijing and Guangzhou is consistently maintained at around 40% during the time from 17<sup>th</sup> to 21<sup>th</sup>. The lower oxidative transformation is related to the lower liquid water content in Beijing, while in Guangzhou it is attributed to the combination of low pollution levels and low cloud water content. Figure 3 shows that Chengdu maintained abundant water vapor conditions from 17<sup>th</sup> to 21<sup>st</sup>, and so does Nanjing from 20<sup>th</sup> to 21<sup>st</sup>. However, the ambient water vapor content is quite low in Guangzhou and Beijing throughout the process and the SO<sub>2</sub> oxidation is much lower than that of Chengdu and Nanjing. In conclusion, the cloud chemistry process can lead to SO<sub>2</sub> column concentration consumption share of more than 60% when cloud water content is abundant, which is also consistent with the observations of Mount Tai by Li (2020).

The impact of cloud chemistry (RT) on surface SO<sub>2</sub> and sulfate in four sites is also shown in Figure 13. The overall trend shows that the peak and valley regions of surface SO<sub>2</sub> consumption and sulfate increase are coincident. The cloud chemical processes of the surface SO<sub>2</sub> oxidation vary greatly between cities in different regions (Fig. 13a). In HPE-2, the percentage of surface SO<sub>2</sub> consumption can reach more than 90% in Chengdu and Nanjing, while it is below 30% in Beijing and Guangzhou, and does not reach 40% until the 22<sup>nd</sup>. Although the percentage of surface SO<sub>2</sub> consumption varies greatly, the increase in the percentage of sulfate does not vary so much between cities. In HPE-2, the increase in surface sulfate in the four cities ranges from 60-95% (Fig. 13b), and the sulfate increase rate interval contains the results summarized by Turnock et al. (2019).

Figure 14 is the variation of vertical profiles of sulfate increase by the cloud chemistry at the four times at 12:00 LST on 20 for HPE-2, at 04:00 LST on 21 for HPE-2, at 04:00 and 12:00 LST on 22 for HPE-3 in Beijing, Nanjing, Chengdu and Guangzhou. It shows that the sulfate produced by the cloud chemistry during this pollution process is concentrated mostly below 5 km in the troposphere, especially under 2 km. Again, less sulfate has been produced in Beijing in vertical than that of others by the cloud chemistry.



#### 4. Summary and conclusions

The cloud chemistry mechanism in WRF/CUACE has been assessed by using the in-situ cloud chemistry observations of SO<sub>2</sub>, O<sub>3</sub>, and H<sub>2</sub>O<sub>2</sub> from Mount Tai in June-July 2015 and 2018. The results show that the mechanism well captures the cloud processes for the oxidation of SO<sub>2</sub>, reducing SO<sub>2</sub> by more than 80% during the cloudy phase, which is in good agreement with the observations.

The cloud chemistry contributions to the changes of SO<sub>2</sub> and sulfate concentrations in NCP, YRD, PRD and SCB regions are assessed by WRF/CUACE. During heavy pollution (HPE-2), the four regions are significantly affected by cloud chemistry, with SCB being the most obvious. The surface SO<sub>2</sub> reduction in SCB is up to 1.0-3.0 ppb and reaches 3.0-10.0 ppb in the high value areas, and surface sulfate concentration is increased by 10.0-30.0 µg/m<sup>3</sup> on average, with a maximum of more than 70.0 µg/m<sup>3</sup>. Most areas in NCP, YRD and PRD have an average SO<sub>2</sub> reduction of 0.5-3.0 ppb and sulfate increase of 5.0-30.0 µg/m<sup>3</sup>. Meanwhile, the Beijing area of NCP has the least impact among the four typical cities of four regions. Although the monthly average impact of cloud chemistry is much weaker in the NCP due to less water vapor in December, the contribution of the southern part of NCP during heavy pollution time is still significant and cannot be ignored. In PRD, the contribution of cloud chemistry is weaker than other regions due to lighter pollution, although there are lots of clouds with abounded liquid water there. In addition, the cloud chemistry increases surface sulfate concentration by 60-95% and reduces surface SO<sub>2</sub> concentration by more than 80% in Beijing, Nanjing, Chengdu and Guangzhou in December during HPE-2, similar to that of previous studies (Turnock et al., 2019; Faloon et al., 2009). Above all, the average contribution of cloud chemistry during HPE-2 is significantly greater than that for DEC. Vertically, the cloud chemistry influence is mainly in the middle and lower troposphere below 2 km for four representative cities in HPE-2. Generally, the cloud chemistry can improve the model performance by reducing the overestimates of SO<sub>2</sub> and underestimates of sulfate.

This paper focuses on the cloud chemical mechanism evaluation, and assessed the contribution of cloud chemistry to SO<sub>2</sub> and sulfate changes. In the future, more mechanisms should be added to improve the cloud chemistry mechanism in CUACE to more accurately simulate SO<sub>2</sub> and sulfate and other

420 aerosol components such as nitrate, ammonium, carbonate, and organic aerosols.

### **Code/data availability**

All source code and data can be accessed by contacting the corresponding authors Sunling Gong ([gongsl@cma.gov.cn](mailto:gongsl@cma.gov.cn)).

### **Authors contribution**

425 CZ and SG put forward the ideas and formulated overarching research goals. JL carried them out and wrote the manuscript with suggestions from all authors. LZ and JZ participated in the scientific interpretation and discussion. JC was assisted with data acquisition and processing. All authors contributed to the discussion and improvement of the manuscript.

### **Competing interests**

430 The authors declare that they have no conflict of interest.

### **Financial support**

This research has been supported by the National Key Project of the Ministry of Science and Technology of China (2022YFC3701205); CMA Innovation Development Project (CXFZ2021J023).

- Alexander, B., Park, R. J., Jacob, D. J., and Gong, S.: Transition metal-catalyzed oxidation of atmospheric sulfur: Global implications for the sulfur budget, *Journal of Geophysical Research: Atmospheres*, 114, <https://doi.org/10.1029/2008jd010486>, 2009.
- Buchard, V., da Silva, A. M., Colarco, P., Krotkov, N., Dickerson, R. R., Stehr, J. W., Mount, G., Spinei, E., Arkinson, H. L., and He, H.: Evaluation of GEOS-5 sulfur dioxide simulations during the Frostburg, MD 2010 field campaign, *Atmos. Chem. Phys.*, 14, 1929-1941, <https://doi.org/10.5194/acp-14-1929-2014>, 2014.
- Binkowski, F. S., and Roselle, S. J.: Models - 3 Community Multiscale Air Quality (CMAQ) model aerosol component 1. Model description, *Journal of Geophysical Research: Atmospheres*, 108, <https://doi.org/10.1029/2001jd001409>, 2003.
- Caffrey, P., Hoppel, W., Frick, G., Pasternack, L., Fitzgerald, J., Hegg, D., Gao, S., Leaitch, R., Shantz, N., Albrechtski, T., and Ambrusko, J.: In-cloud oxidation of SO<sub>2</sub> by O<sub>3</sub> and H<sub>2</sub>O<sub>2</sub>: Cloud chamber measurements and modeling of particle growth, *Journal of Geophysical Research: Atmospheres*, 106, 27587-27601, <https://doi.org/10.1029/2000jd900844>, 2001.
- Chang, J. S., Brost, R. A., Isaksen, I. S. A., Madronich, S., Middleton, P., Stockwell, W. R., and Walcek, C. J.: A three-dimensional eulerian acid deposition model physical concepts and formulation, *Journal of Geophysical Research: Atmospheres*, 92, 14,681-614,700, <https://doi.org/10.1029/jd092id12p14681>, 1987.
- Chapman, E. G., Gustafson, W. I., Easter, R. C., Barnard, J. C., and Fast, J. D.: Coupling aerosol-cloud-radiative processes in the WRF-Chem model: Investigating the radiative impact of elevated point sources, *Atmos. Chem. Phys.*, 9, 945-964, <https://doi.org/10.5194/acp-9-945-2009>, 2009.
- Chameides, W. L.: The photochemistry of a remote marine stratiform cloud, *J. Geophys. Res.*, 89, 4739-4756, <https://doi.org/10.1029/JD089iD03p04739>, 1984.

- Charlson, R. J., Schwartz, S. E., Hales, J. M., Cess, R. D., Coakley, A., JR., Hansen, J. E., and Hofmann,  
460 D. J.: Climate forcing by anthropogenic aerosols, *Science*, 255, 423-423,  
<https://doi.org/10.1126/science.255.5043.423>, 1992.
- Emery, C., Tai, E., and Yarwood, G.: Enhanced meteorological modeling and performance evaluation for  
two Texas ozone episodes, *Biology*, Corpus ID: 127579774, 2001.
- Cheng, Y., Zheng, G., Wei, C., Mu, Q., Zheng, B., Wang, Z., Gao, M., Zhang, Q., He, K., and  
465 Carmichael, G.: Reactive nitrogen chemistry in aerosol water as a source of sulfate during haze events in  
China, *Science Advances*, <https://doi.org/10.1126/sciadv.1601530>, 2016.
- Dovrou, E., Rivera-Rios, J. C., Bates, K. H., and Keutsch, F. N.: Sulfate Formation via Cloud Processing  
from Isoprene Hydroxyl Hydroperoxides (ISOPOOH), *Environ Sci Technol*, 53, 12476-12484,  
<https://doi.org/10.1021/acs.est.9b04645>, 2019.
- 470 Ervens, B.: Modeling the Processing of Aerosol and Trace Gases in Clouds and Fogs, *Chemical Reviews*,  
115, 4157-4198, <https://doi.org/10.1021/cr5005887>, 2015.
- Faloona, I.: Sulfur processing in the marine atmospheric boundary layer: A review and critical  
assessment of modeling uncertainties, *Atmospheric Environment*, 43(18), 2841-2854,  
<https://doi.org/10.1016/j.atmosenv.2009.02.043>, 2009.
- 475 Faloona, I., Conley, S. A., Blomquist, B., Clarke, A. D., Kapustin, V., Howell, S., Lenschow, D. H., and  
Bandy, A. R.: Sulfur dioxide in the tropical marine boundary layer: dry deposition and heterogeneous  
oxidation observed during the Pacific Atmospheric Sulfur Experiment, *Journal of Atmospheric  
Chemistry*, 63, 13-32, <https://doi.org/10.1007/s10874-010-9155-0>, 2010.
- Gao, M., Carmichael, G. R., Wang, Y., Ji, D., Liu, Z., and Wang, Z.: Improving simulations of sulfate  
480 aerosols during winter haze over Northern China: the impacts of heterogeneous oxidation by NO<sub>2</sub>,  
*Frontiers of Environmental Science & Engineering*, 10, 11, <https://doi.org/10.1007/s11783-016-0878-2>,  
2016.

Ge, W., Liu, J., Xiang, S., Zhou, Y., Zhou, J., Hu, X., Ma, J., Wang, X., Wan, Y., Hu, J., Zhang, Z., Wang, X., Tao, S.: Improvement and Uncertainties of Global Simulation of Sulfate Concentration and Radiative  
485 Forcing in CESM2, <https://doi.org/10.1002/essoar.10512154.1>, 2022.

Ge, W., Liu, J., Yi, K., Xu, J., Zhang, Y., Hu, X., Ma, J., Wang, X., Wan, Y., Hu, J., Zhang, Z., Wang, X., and Tao, S.: Influence of atmospheric in-cloud aqueous-phase chemistry on global simulation of SO<sub>2</sub> in CESM2, *Atmos. Chem. Phys.*, <https://doi.org/10.5194/acp-2021-406>, 2021.

Georgiou, G. K., Christoudias, T., Proestos, Y., Kushta, J., Hadjinicolaou, P., and Lelieveld, J.: Air  
490 quality modelling in the summer over the eastern Mediterranean using WRF-Chem: chemistry and aerosol mechanism intercomparison, *Atmos. Chem. Phys.*, 18, 1555-1571, <https://doi.org/10.5194/acp-18-1555-2018>, 2018.

Gen, M., Zhang, R., Huang, D. D., Li, Y., Chan, C. K.: Heterogeneous SO<sub>2</sub> Oxidation in Sulfate Formation by Photolysis of Particulate Nitrate, *Environ. Sci. Technol*, 6 (2), 86–91,  
495 <https://doi.org/10.1021/acs.estlett.8b00681>, 2019a.

Gen, M., Zhang, R., Huang, D. D., Li, Y., and Chan, C. K.: Heterogeneous Oxidation of SO(2) in Sulfate Production during Nitrate Photolysis at 300 nm: Effect of pH, Relative Humidity, Irradiation Intensity, and the Presence of Organic Compounds, *Environ Sci Technol*, 53, 8757-8766, <https://doi.org/10.1021/acs.est.9b01623>, 2019b.

500 Gong, S., and Zhang, X.: CUACE/Dust – an integrated system of observation and modeling systems for operational dust forecasting in Asia, *Atmospheric Chemistry and Physics*, 8, 2333-2340, <https://doi.org/10.5194/acp-8-2333-2008>, 2008.

Gong, S. L., Barrie, L. A., Blanchet, J.-P., von Salzen, K., Lohmann, U., Lesins, G., Spacek, L., Zhang, L. M., Girard, E., Lin, H., Leaitch, R., Leighton, H., Chylek, P., and Huang, P.: Canadian Aerosol  
505 Module: A size-segregated simulation of atmospheric aerosol processes for climate and air quality models 1. Module development, *Journal of Geophysical Research: Atmospheres*, 108, <https://doi.org/10.1029/2001jd002002>, 2003.

Guo, J., Wang, Y., Shen, X., Wang, Z., Lee, T., Wang, X., Li, P., Sun, M., Jeffrey, L., Collett, J., Wang, W., and Wang, T.: Characterization of cloud water chemistry at Mount Tai, China: Seasonal variation, anthropogenic impact, and cloud processing, *Atmospheric Environment*, 60, 467-476, <https://doi.org/10.1016/j.atmosenv.2012.07.016>, 2012.

Guo, S., Hu, M., Zamora, M. L., Peng, J., Shang, D., Zheng, J., Du, Z., Wu, Z., Shao, M., Zeng, L., Molina, M. J., and Zhang, R.: Elucidating severe urban haze formation in China, *Proceedings of the National Academy of Sciences*, 111, 17373-17378, <https://doi.org/10.1073/pnas.1419604111>, 2014.

Harris, E., Sinha, B., van Pinxteren, D., Tilgner, A., Fomba, K. W., Schneider, J., Roth, A., Gnauk, T., Fahlbusch, B., Mertes, S., Lee, T., Collett, J., Foley, S., Borrmann, S., Hoppe, P., and Herrmann, H.: Enhanced role of transition metal ion catalysis during in-cloud oxidation of SO<sub>2</sub>, *Science*, 340, 727-730, <https://doi.org/10.1126/science.1230911>, 2013.

He, J., Zhang, Y., Glotfelty, T., He, R., Bennartz, R., Rausch, J., and Sartelet, K.: Decadal simulation and comprehensive evaluation of CESM/CAM5.1 with advanced chemistry, aerosol microphysics, and aerosol-cloud interactions, *Journal of Advances in Modeling Earth Systems*, 7, 110-141, <https://doi.org/10.1002/2014ms000360>, 2015.

Huang, L., An, J., Koo, B., Yarwood, G., Yan, R., Wang, Y., Huang, C., and Li, L.: Sulfate formation during heavy winter haze events and the potential contribution from heterogeneous SO<sub>2</sub> + NO<sub>2</sub> reactions in the Yangtze River Delta region, China, *Atmos. Chem. Phys.*, 19, 14311–14328, <https://doi.org/10.5194/acp-19-14311-2019>, 2019.

Hung, H. M., Hsu, M. N., and Hoffmann, M. R.: Quantification of SO<sub>2</sub> Oxidation on Interfacial Surfaces of Acidic Micro-Droplets: Implication for Ambient Sulfate Formation, *Environ Sci Technol*, 52, 9079-9086, <https://doi.org/10.1021/acs.est.8b01391>, 2018.

Kotarba, A. Z.: Calibration of global MODIS cloud amount using CALIOP cloud profiles, *Atmospheric Measurement Techniques*, 13, 4995-5012, <https://doi.org/10.5194/amt-13-4995-2020>, 2020.

Iibusuki, T., and Takeuchi, K.: Sulfur dioxide oxidation by oxygen catalyzed by mixtures of manganese(II) and iron(III) in aqueous solutions at environmental reaction conditions, *Atmospheric Environment*, 21, 1555-1560, [https://doi.org/10.1016/0004-6981\(87\)90317-9](https://doi.org/10.1016/0004-6981(87)90317-9), 1987.

535 Ivanova, I. T., and Leighton, H. G.: Aerosol-Cloud Interactions in a Mesoscale Model. Part II: Sensitivity to Aqueous-Phase Chemistry, *Journal of the Atmospheric Sciences*, 65, 309-330, <https://doi.org/10.1175/2007JAS2276.1>, 2008.

Leighton, H. G., and Ivanova, I. T.: Aerosol-Cloud Interactions in a Mesoscale Model. Part I: Sensitivity to Activation and Collision-Coalescence, *Journal of the Atmospheric Sciences*, 65, 289-308, 540 <https://doi.org/10.1175/2007jas2207.1>, 2008.

Lelieveld, J., and Heintzenberg, J.: Sulfate cooling effect on climate through in-cloud oxidation of anthropogenic SO<sub>2</sub>, *Science*, 285, 117-120, <https://doi.org/10.1126/science.258.5079.117>, 1992.

Leighton, H. G., Yau M. K., Macdonald, A. M., Pitre, J. S., and Giles, A.: A numerical simulation of the chemistry of a rainband, *Atmospheric Environment*, 24, 1211-1217, [https://doi.org/10.1016/0960-1686\(90\)90086-3](https://doi.org/10.1016/0960-1686(90)90086-3), 1990. 545

Li, J. R.: Microphysical Characteristics and S(IV) Multiphase Chemical Reaction Mechanism of Orographic Clouds, Ph.D. thesis, Fudan University, 127pp, 2020.

Li, J., Wang, X., Chen, J., Zhu, C., Li, W., Li, C., Liu, L., Xu, C., Wen, L., Xue, L., Wang, W., Ding, A., and Herrmann, H.: Chemical composition and droplet size distribution of cloud at the summit of Mount 550 Tai, China, *Atmos. Chem. Phys.*, 17, 9885-9896, <https://doi.org/10.5194/acp-17-9885-2017>, 2017.

Li, J., Zhu, C., Chen, H., Fu, H., Xiao, H., Wang, X., Herrmann, H., and Chen, J.: A More Important Role for the Ozone - S(IV) Oxidation Pathway Due to Decreasing Acidity in Clouds, *Journal of Geophysical Research: Atmospheres*, 125, <https://doi.org/10.1029/2020jd033220>, 2020a.

Li, J., Zhu, C., Chen, H., Zhao, D., Xue, L., Wang, X., Li, H., Liu, P., Liu, J., Zhang, C., Mu, Y., Zhang,

555 W., Zhang, L., Herrmann, H., Li, K., Liu, M., and Chen, J.: The evolution of cloud and aerosol  
microphysics at the summit of Mt. Tai, China, *Atmos. Chem. Phys.*, 20, 13735-13751,  
<https://doi.org/10.5194/acp-20-13735-2020>, 2020b.

Li, M., Liu, H., Geng, G., Hong, C., Liu, F., Song, Y., Tong, D., Zheng, B., Cui, H., Man, H., Zhang, Q.,  
and He, K.: Anthropogenic emission inventories in China: a review, *Natl. Sci. Rev.*, 4, 834-866,  
560 <https://doi.org/10.1093/nsr/nwx150>, 2017.

Liu, S. C., McKeen, S. A., Hsie, E.-Y., Lin, X., Kelly, K. K., Bradshaw, J. D., Sandholm, S. T., Browell,  
E. V., Gregory, G. L., Sachse, G. W., Bandy, A. R., Thornton, D. C., Blake, D. R., Rowland, F. S.,  
Newell, R., Heikes, B. G., Singh, H., and R. W. Talbot: Model study of tropospheric trace species  
distributions during PEM-WEST A, *Journal of Geophysical Research: Atmospheres*, 101,  
565 <https://doi.org/10.148-0227/96/95JD-02277505.00>, 1996.

Li, P. F.: Fog Water Chemistry and Fog-Haze Transformation in Shanghai, Fudan University, Ph.D.  
thesis, 145pp.

Liu, T., Chan, A. W. H., and Abbatt, J. P. D.: Multiphase Oxidation of Sulfur Dioxide in Aerosol  
Particles: Implications for Sulfate Formation in Polluted Environments, *Environ Sci Technol*, 55, 4227-  
570 4242, <https://doi.org/10.1021/acs.est.0c06496>, 2021.

Maahs, H. G.: Kinetics and Mechanism of the Oxidation of S(IV) by Ozone in Aqueous Solution With  
Particular Reference to SO<sub>2</sub> Conversion in Nonurban Tropospheric Clouds, *Journal of Geophysical  
Research Oceans*, 88, 10721-10732, <https://doi.org/10.1029/JC088iC15p10721>, 1983.

Martin, G. M., Johnson D. W., and Spice A., The measurement and parameterization of effective radius  
575 in warm stratocumulus cloud, *J. Atmos. Sci.*, 51, 1823-1842, [https://doi.org/10.1175/1520-0469\(1994\)051<1823:TMAPOE>2.0.CO;2](https://doi.org/10.1175/1520-0469(1994)051<1823:TMAPOE>2.0.CO;2), 1994.

Martin, L. R., and Good, T. W.: Catalyzed oxidation of sulfur dioxide in solution: The iron-manganese  
synergism, *Atmospheric Environment*, 25, 2395-2399, [https://doi.org/10.1016/0960-1686\(91\)90113-L](https://doi.org/10.1016/0960-1686(91)90113-L),



1991.

580 Menut, L., Bessagnet, B., Khvorostyanov, D., Beekmann, M., Colette, A., Coll, I., Curci, G., Foret, G.,  
Hodzic, A., Mailler, S., Meleux, F., Monge, J. L., Pison, I., Turquety, S., Valari, M., Vautard, R., and  
Vivanco, M. G.: Regional atmospheric composition modeling with CHIMERE, *Geoscientific Model  
Development*, 6, 981-1028, <https://doi.org/10.5194/gmdd-6-203-2013>, 2013.

Molina, L. T, and Molina, M. J.: Air Quality in the Mexico Megacity: An Integrated Assessment,  
585 Alliance for Global Sustainability Bookseries, <https://doi.org/10.1007/978-94-010-0454-1>, 2002.

Park, R. J., and Jacob, D. J.: Sources of carbonaceous aerosols over the United States and implications  
for natural visibility, *Journal of Geophysical Research*, 108, <https://doi.org/10.1029/2002jd003190>, 2003.

Pye, H. O. T., Nenes, A., Alexander, B., Ault, A. P., Barth, M. C., Clegg, S. L., Jr., J. L. C., Fahey, K. M.,  
Hennigan, C. J., Herrmann, H., Kanakidou, M., Kelly, J. T., Ku, I.-T., McNeill, V. F., Riemer, N.,  
590 Schaefer, T., Shi, G., Tilgner, A., Walker, J. T., Wang, T., Weber, R., Xing, J., Zaveri, R. A., and Zuend, a.  
A.: Havalala O. T. Pye The acidity of atmospheric particles and clouds, *Atmos. Chem. Phys.*, 20, 4809-  
4888, <https://doi.org/10.5194/acp-20-4809-2020>, 2020.

Ramanathan, V., Crutzen, P. J., Kiehl, J. T., and Rosenfeld, D.: Aerosols, climate, and the hydrological  
cycle, *Science*, 294, 2119-2124, <https://doi.org/10.1126/science.1064034>, 2001.

595 Ravishankara, A. R.: Heterogeneous and Multiphase Chemistry in the Troposphere, *Science*, 276, 1058-  
1065, <https://doi.org/10.1126/science.276.5315.1058>, 1997.

Ren, Y., Ding, A., Wang, T., Shen, X., Guo, J., Zhang, J., Wang, Y., Xu, P., Wang, X., and Gao, J.:  
Measurement of gas-phase total peroxides at the summit of Mount Tai in China, *Atmospheric  
Environment*, 43, 1702-1711, <https://doi.org/10.1016/j.atmosenv.2008.12.020>, 2009.

600 Sha, T., Ma, X., Jia, H., Tian, R., Chang, Y., Cao, F., and Zhang, Y.: Aerosol chemical component:  
Simulations with WRF-Chem and comparison with observations in Nanjing, *Atmospheric Environment*,

218, <https://doi.org/10.1016/j.atmosenv.2019.116982>, 2019.

Shen, X., Lee, T., Guo, J., Wang, X., Li, P., Xu, P., Wang, Y., Ren, Y., Wang, W., Wang, T., Li, Y., Carn, S. A., and Collett, J. L.: Aqueous phase sulfate production in clouds in eastern China, *Atmospheric Environment*, 62, 502-511, <https://doi.org/10.1016/j.atmosenv.2012.07.079>, 2012.

Shimadera, H., Kondo, A., Shrestha, K. L., Kaga, A., and Inoue, Y.: Annual sulfur deposition through fog, wet and dry deposition in the Kinki Region of Japan - ScienceDirect, *Atmospheric Environment*, 45, 6299-6308, <https://doi.org/10.1016/j.atmosenv.2011.08.055>, 2011.

Sielski, J., Kazirod-Wolski, K., Jozwiak, M. A., and Jozwiak, M.: The influence of air pollution by PM<sub>2.5</sub>, PM<sub>10</sub> and associated heavy metals on the parameters of out-of-hospital cardiac arrest, *Sci Total Environ*, 788, 147541, <https://doi.org/10.1016/j.scitotenv.2021.147541>, 2021.

Song, S., Nenes, A., Gao, M., Zhang, Y., Liu, P., Shao, J., Ye, D., Xu, W., Lei, L., Sun, Y., Liu, B., Wang, S., and McElroy, M. B.: Thermodynamic Modeling Suggests Declines in Water Uptake and Acidity of Inorganic Aerosols in Beijing Winter Haze Events during 2014/2015–2018/2019, *Environmental Science & Technology Letters*, 6, 752-760, <https://doi.org/10.1021/acs.estlett.9b00621>, 2019.

Terrenoire, E., Bessagnet, B., Rouil, L., Tognet, F., Pirovano, G., Létinois, L., Beauchamp, M., Colette, A., Thunis, P., Amann, M., and Menut, L.: High-resolution air quality simulation over Europe with the chemistry transport model CHIMERE, *Geoscientific Model Development*, 8, 21-42, <https://doi.org/10.5194/gmd-8-21-2015>, 2015.

Tie, X.: Assessment of the global impact of aerosols on tropospheric oxidants, *Journal of Geophysical Research*, 110, <https://doi.org/10.1029/2004jd005359>, 2005.

Tremblay, A., and Leighton, H.: A Three-Dimensional Cloud Chemistry Model, *Journal of Climate & Applied Meteorology*, 25, 652-671, [https://doi.org/10.1016/1352-2310\(96\)00063-5](https://doi.org/10.1016/1352-2310(96)00063-5), 1986.

Tuccella, P., Curci, G., Visconti, G., Bessagnet, B., Menut, L., Park, R.: Modeling of gas and aerosol

- 625 with WRF/Chem over Europe: Evaluation and sensitivity study, *Journal of Geophysical Research*, 117, <https://doi.org/10.1029/2011JD016302>, 2012.
- Turnock, S. T., Mann, G. W., Woodhouse, M. T., Dalvi, M., O'Connor, F. M., Carslaw, K. S., and Sprackle, D. V.: The Impact of Changes in Cloud Water pH on Aerosol Radiative Forcing, *Geophysical Research Letters*, 46, 4039 – 4048, <https://doi.org/10.1029/2019GL082067>, 2019.
- 630 Twomey S.: Aerosols, clouds and radiation, *Atmospheric Environment. part A. general Topics*, 25, 2435-2442, [https://doi.org/10.1016/0960-1686\(91\)90159-5](https://doi.org/10.1016/0960-1686(91)90159-5), 1991.
- Twomey, S. A., Piepgrass, M., and Wolfe, T. L.: An assessment of the impact of pollution on the global cloud albedo, *Tellus B: Chemical and Physical Meteorology*, 36B, 356-366, <https://doi.org/10.1111/j.1600-0889.1984.tb00254.x>, 1984.
- 635 von Salzen, K., Leighton, H. G., Ariya, P. A., Barrie, L. A., Gong, S. L., Blanchet, J. P., Spacek, L., Lohmann, U., and Kleinman, L. I.: Sensitivity of sulphate aerosol size distributions and CCN concentrations over North America to SO<sub>x</sub> emissions and H<sub>2</sub>O<sub>2</sub> concentrations, *Journal of Geophysical Research: Atmospheres*, 105, 9741-9765, <https://doi.org/10.1029/2000jd900027>, 2000.
- 640 Wang, G., Zhang, R., Gomez, M. E., Yang, L., Levy Zamora, M., Hu, M., Lin, Y., Peng, J., Guo, S., Meng, J., Li, J., Cheng, C., Hu, T., Ren, Y., Wang, Y., Gao, J., Cao, J., An, Z., Zhou, W., Li, G., Wang, J., Tian, P., Marrero-Ortiz, W., Secret, J., Du, Z., Zheng, J., Shang, D., Zeng, L., Shao, M., Wang, W., Huang, Y., Wang, Y., Zhu, Y., Li, Y., Hu, J., Pan, B., Cai, L., Cheng, Y., Ji, Y., Zhang, F., Rosenfeld, D., Liss, P. S., Duce, R. A., Kolb, C. E., and Molina, M. J.: Persistent sulfate formation from London Fog to Chinese haze, *Proc Natl Acad Sci U S A*, 113, 13630-13635, <https://doi.org/10.1073/pnas.1616540113>,  
645 2016.
- Wang, H., Shi, G. Y., Zhang, X. Y., Gong, S. L., Tan, S. C., Chen, B., Che, H. Z., and Li, T.: Mesoscale modelling study of the interactions between aerosols and PBL meteorology during a haze episode in China Jing-Jin-Ji and its near surrounding region - Part 2: Aerosols' radiative feedback effects, *Atmos. Chem. Phys.*, 15, 6(2015-03-23), 14, 3277-3287, <https://doi.org/10.5194/acp-15-3257-2015>, 2015.

650 Wang, J., Li, J., Ye, J., Zhao, J., Wu, Y., Hu, J., Liu, D., Nie, D., Shen, F., Huang, X., Huang, D. D., Ji, D., Sun, X., Xu, W., Guo, J., Song, S., Qin, Y., Liu, P., Turner, J. R., Lee, H. C., Hwang, S., Liao, H., Martin, S. T., Zhang, Q., Chen, M., Sun, Y., Ge, X., and Jacob, D. J.: Fast sulfate formation from oxidation of SO<sub>2</sub> by NO<sub>2</sub> and HONO observed in Beijing haze, *Nature Communications*, 11, <https://doi.org/10.1038/s41467-020-16683-x>, 2020.

655 Wang, S., Zhou, S., Tao, Y., Tsui, W. G., Ye, J., Yu, J. Z., Murphy, J. G., McNeill, V. F., Abbatt, J. P. D., and Chan, A. W. H.: Organic Peroxides and Sulfur Dioxide in Aerosol: Source of Particulate Sulfate, *Environ Sci Technol*, 53, 10695-10704, <https://doi.org/10.1021/acs.est.9b02591>, 2019.

Wei, Y., Chen, X., Chen, H., Li, J., Wang, Z., Yang, W., Ge, B., Du, H., Hao, J., Wang, W., Li, J., Sun, Y., and Huang, H.: IAP-AACM v1.0: a global to regional evaluation of the atmospheric chemistry model in  
660 CAS-ESM, *Atmos. Chem. Phys.*, 19, 8269-8296, <https://doi.org/10.5194/acp-19-8269-2019>, 2019.

Xie, Y., Dai, H., Zhang, Y., Wu, Y., Hanaoka, T., and Masui, T.: Comparison of health and economic impacts of PM<sub>2.5</sub> and ozone pollution in China, *Environ Int*, 130, 104881, <https://doi.org/10.1016/j.envint.2019.05.075>, 2019.

Yao, S., Wang, Q., Zhang, J., and Zhang, R.: Characteristics of Aerosol and Effect of Aerosol-Radiation-  
665 Feedback in Handan, an Industrialized and Polluted City in China in Haze Episodes, *Atmosphere*, 12, 670, <https://doi.org/10.3390/atmos12060670>, 2021.

Yao, M., Zhao, Y., Hu, M., Huang, D., Wang, Y., Yu, J. Z., and Yan, N.: Multiphase Reactions between Secondary Organic Aerosol and Sulfur Dioxide: Kinetics and Contributions to Sulfate Formation and Aerosol Aging, *Environmental Science & Technology Letters*, 6, 768-774,  
670 <https://doi.org/10.1021/acs.estlett.9b00657>, 2019.

Ye, C., Xue, C., Zhang, C., Ma, Z., Liu, P., Zhang, Y., Liu, C., Zhao, X., Zhang, W., He, X., Song, Y., Liu, J., Wang, W., Sui, B., Cui, R., Yang, X., Mei, R., Chen, J., and Mu, Y.: Atmospheric Hydrogen Peroxide H<sub>2</sub>O<sub>2</sub> at the Foot and Summit of Mt Tai Variations Sources, *Journal of Geophysical Research: Atmospheres*, 126, <https://doi.org/10.1029/2020JD033975>, 2021.

675 Ye, J., Abbatt, J. P. D., and Chan, A. W. H.: Novel pathway of SO<sub>2</sub> oxidation in the atmosphere: reactions with monoterpene ozonolysis intermediates and secondary organic aerosol, *Atmos. Chem. Phys.*, 18, 5549-5565, <https://doi.org/10.5194/acp-18-5549-2018>, 2018.

Yuan, D. M., and Ma, X. H.: The severe haze process in 16 – 21 December 2016 and associated atmospheric circulation anomalies [J]. *Climatic and Environmental Research (in Chinese)*, 22 (6): 757-680 764, <https://doi.org/10.3878/j.issn.1006-9585.2017.17029>, 2017.

Zhang, L., Gong, S., Zhao, T. L., Zhou, C. H., and Zhang, X. Y.: Development of WRF/CUACE v1.0 model and its preliminary application in simulating air quality in China, *Geoscientific Model Development*, <https://doi.org/10.5194/gmd-14-703-2021>, 2021.

Zhang, X. Y., Wang, Y. Q., Niu, T., Zhang, X. C., Gong, S. L., Zhang, Y. M., and Sun, J. Y.: Atmospheric 685 aerosol compositions in China: spatial/temporal variability, chemical signature, regional haze distribution and comparisons with global aerosols, *Atmos. Chem. Phys.*, 12, 779-799, <https://doi.org/10.5194/acp-12-779-2012>, 2012.

Zheng, B., Tong, D., Li, M., Liu, F., Hong, C., Geng, G., Li, H., Li, X., Peng, L., Qi, J., Yan, L., Zhang, Y., Zhao, H., Zheng, Y., He, K., and Zhang, Q.: Trends in China's anthropogenic emissions since 2010 as 690 the consequence of clean air actions, *Atmos. Chem. Phys.*, 18, 14095-14111, <https://doi.org/10.5194/acp-18-14095-2018>, 2018.

Zheng, B., Zhang, Q., Zhang, Y., He, K. B., Wang, K., Zheng, G. J., Duan, F. K., Ma, Y. L., and Kimoto, T.: Heterogeneous chemistry: a mechanism missing in current models to explain secondary inorganic aerosol formation during the January 2013 haze episode in North China, *Atmos. Chem. Phys.*, 14, 2031-695 2049, <https://doi.org/10.5194/acp-15-2031-2015>, 2015.

Zhou, C. H., Gong, S., Zhang, X. Y., Liu, H. L., Xue, M., Cao, G. L., An, X. Q., and Che, H. Z.: Towards the improvements of simulating the chemical and optical properties of Chinese aerosols using an online coupled model - CUACE/Aero, *Chemical and physical and meteorology*, <https://doi.org/10.3402/tellusb.v64i0.18965>, 2012.

700 Zhou, C. H., Zhang, X. Y., Gong, S., Wang, Y. Q., and Xue, M.: Improving aerosol interaction with  
clouds and precipitation in a regional chemical weather modeling system, *Atmospheric Chemistry and  
Physics*, 16, 145-160, <https://doi.org/10.5194/acp-16-145-2016>, 2016.

Zhou Y., Gong S., Zhou C., Zhang L., He J., Wang Y., Ji D., Feng J., Mo J., Ke H.: A new  
parameterization of uptake coefficients for heterogeneous reactions on multi-component atmospheric  
705 aerosols, *Science of the Total Environment*, 781, <https://doi.org/10.1016/j.scitotenv.2021.146372>, 2021.

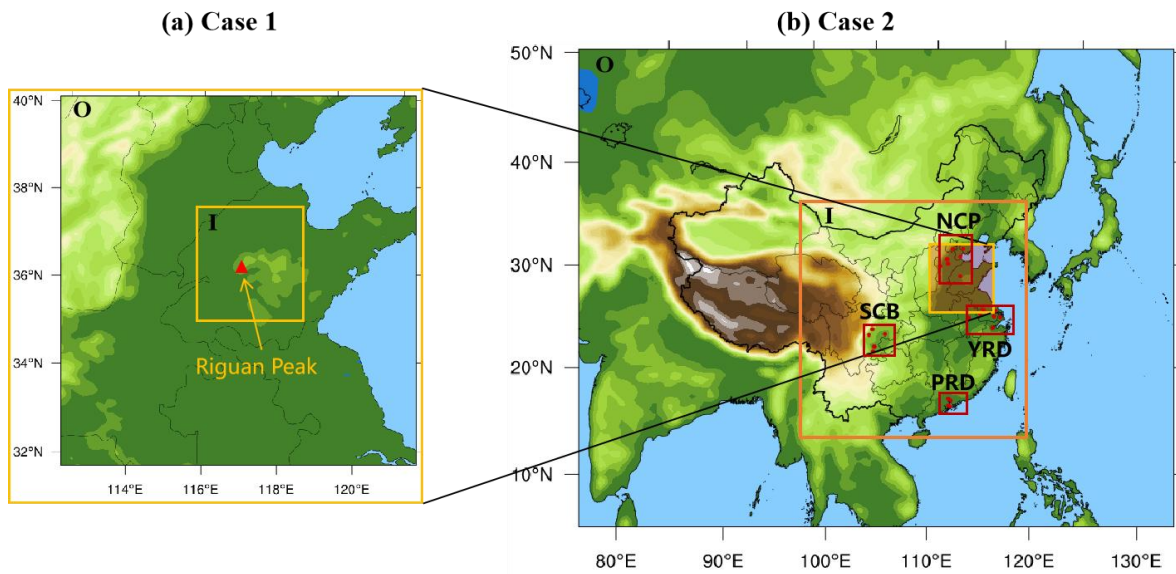


**Figure 1. Model nesting domains and target regions: (a) domain for the Case 1. The red triangle is the Mount Tai site, (b) nesting domains for regional assessment for Case 2. Red dots are where the surface observations of air pollutants are. The target four regions are NCP for the North China Plain, YRD for the Yangtze River Delta, PRD for the Pearl River Delta and SCB for the Sichuan Basin.**

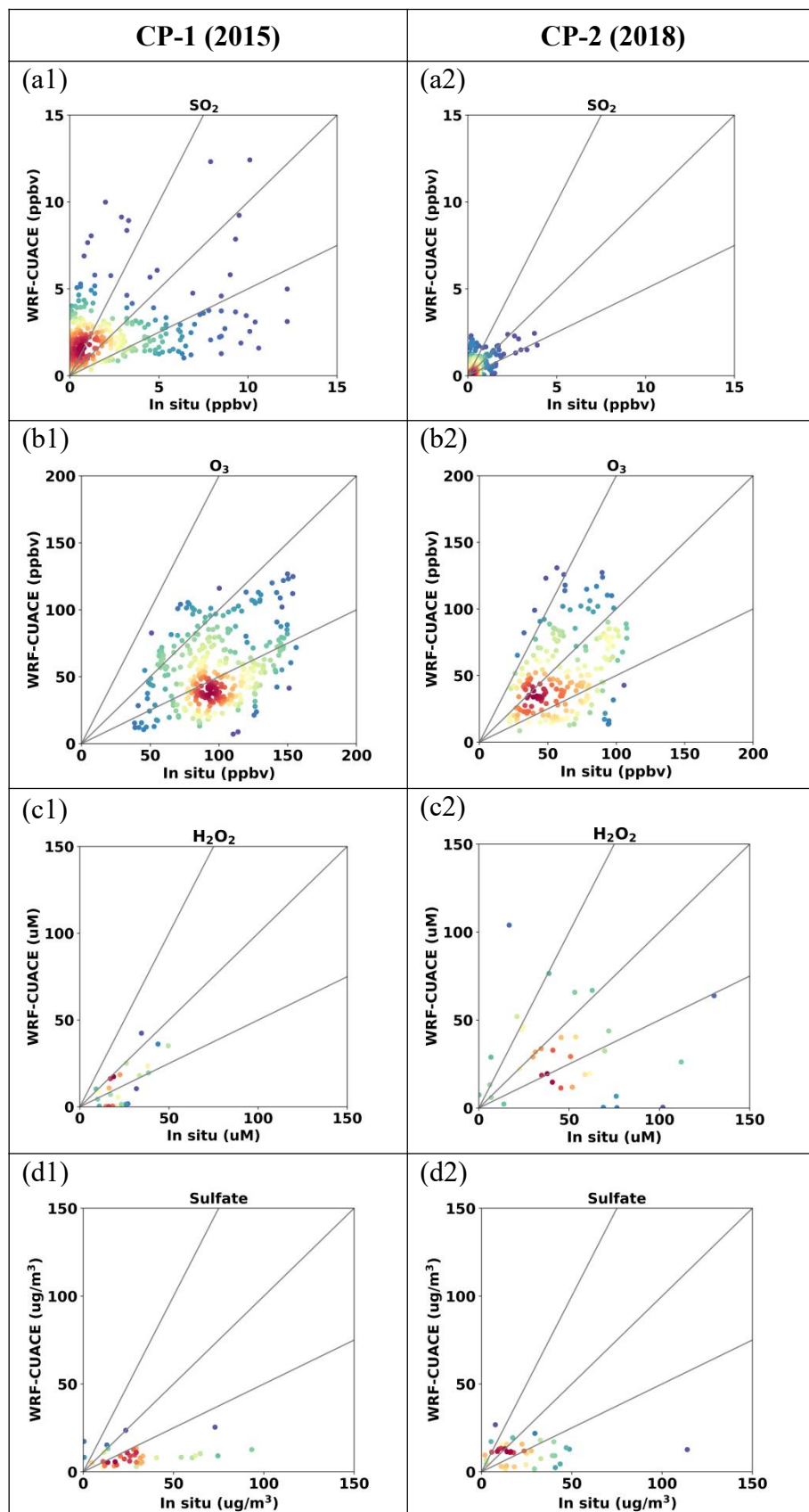


**Figure 2. Scatter plots of hourly SO<sub>2</sub> (a1, a2), O<sub>3</sub> (b1, b2), H<sub>2</sub>O<sub>2</sub> (c1, c2) and sulfate (d1, d2) concentrations between WRF/CUACE and in situ observations at Mount Tai in CP-1 and CP-2. Units: SO<sub>2</sub> and O<sub>3</sub> (ppbv), H<sub>2</sub>O<sub>2</sub> (μM), and Sulfate (μg/m<sup>3</sup>).**



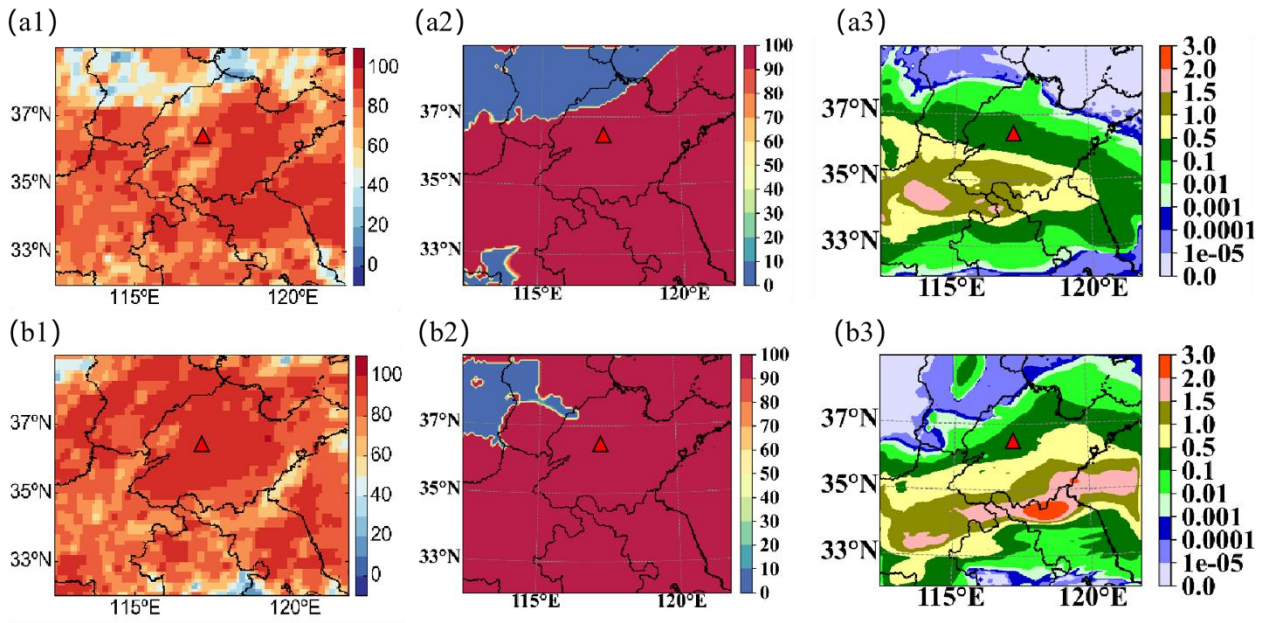


**Figure 3.:** The cloud image of FY2G, (a1, b1, Units: %), the cloud fraction by WRF/CUACE.(a2, b2, Units: %) and the column liquid water content by WRF/CUACE (a3, b3, Units: kg/m<sup>2</sup>). (a) is for 8:00 LST on 24 June, (b) is for 8:00 LST on 25 June.

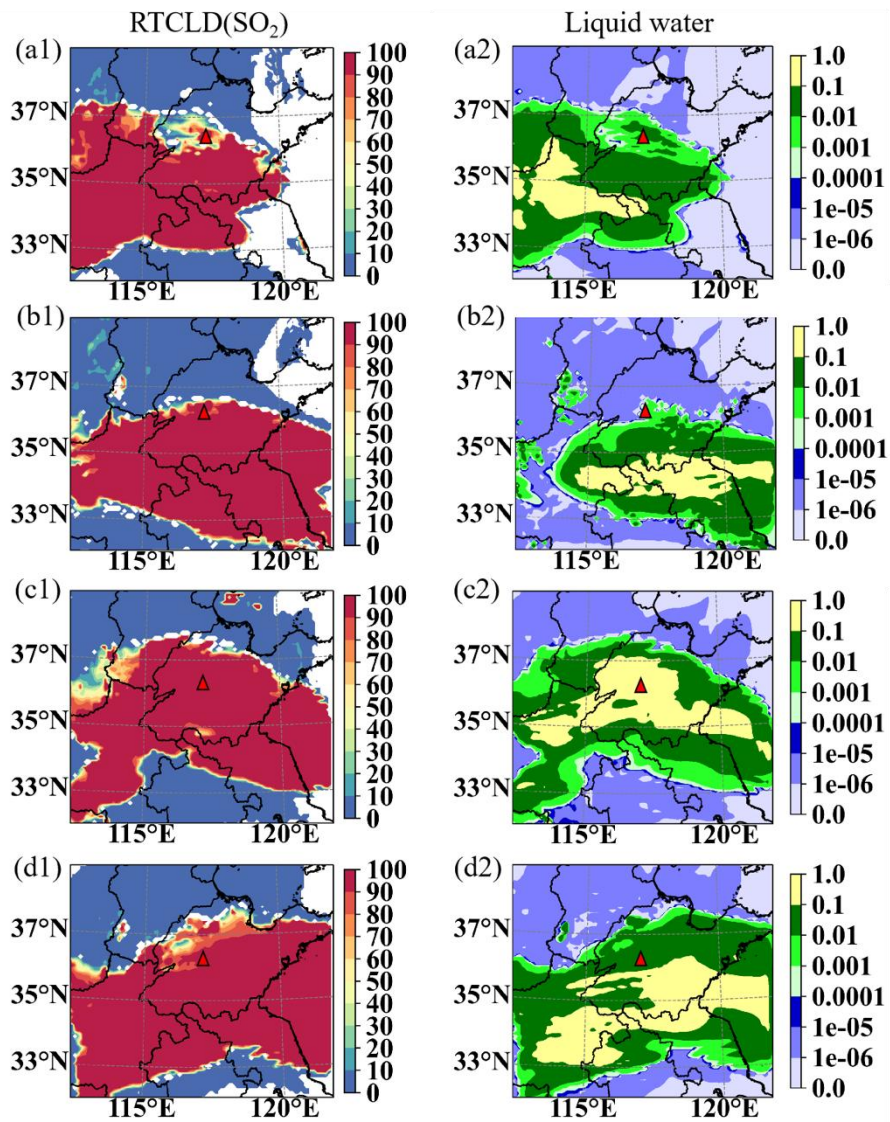


**Figure 4. Distributions of SO<sub>2</sub> oxidation rate (a1, b1, c1 and d1, Units: %) and the liquid water content (a2, b2, c2 and d2, Units: g/kg) by WRF/CUACE, where (a) is for 2:00 LST on 24 June, (b) is for 8:00 LST on 24 June, (c) is for 2:00 LST on 25 June and (d) is for 8:00 LST on 25 June.**



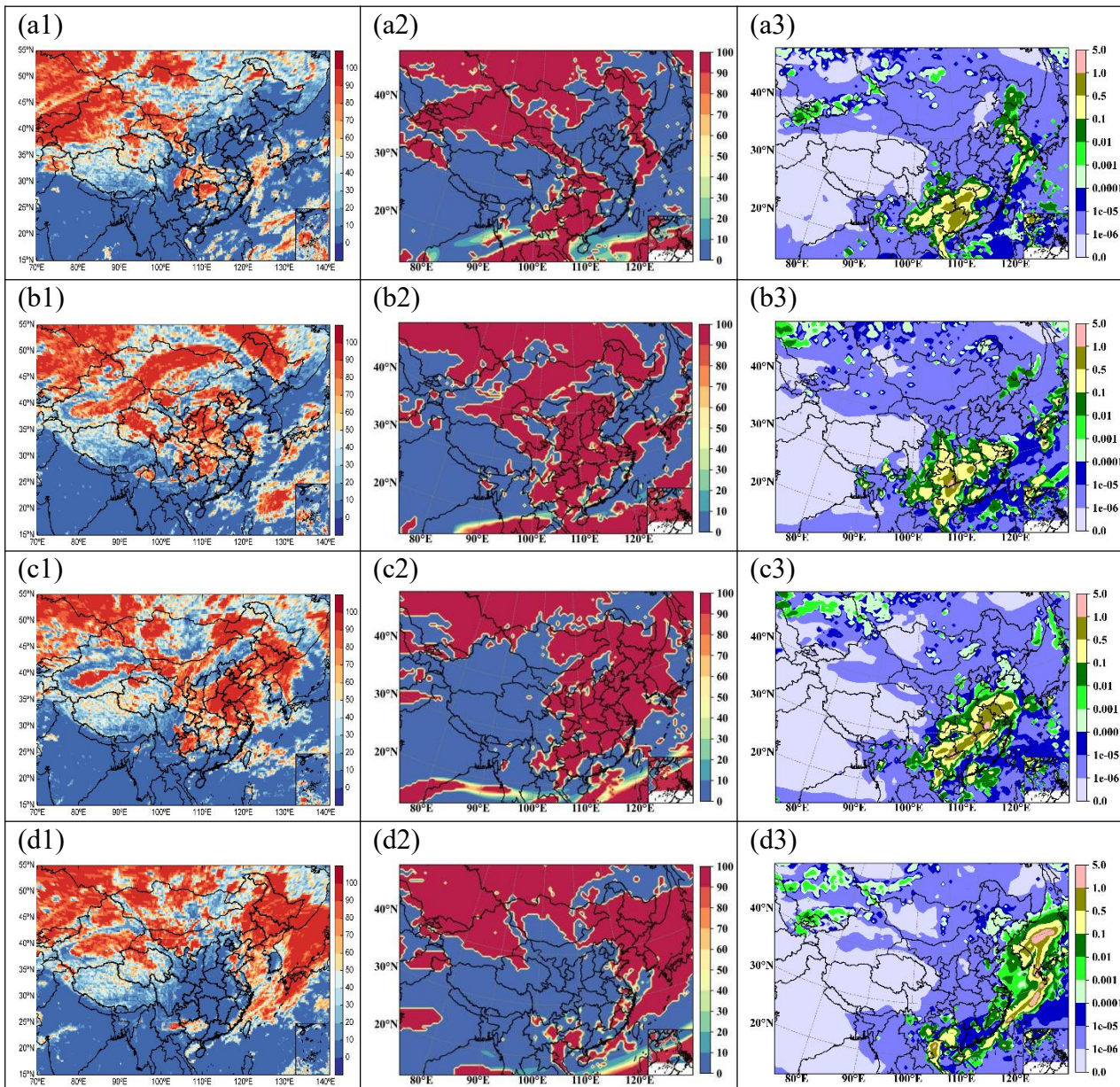


**Figure 5.** The cloud image of FY-2G (a1, b1, c1, d1, Units: %), the column cloud of WRF/CUACE (a2, b2, c2, d2, Units: %) and the column liquid water content of WRF/CUACE (a3, b3, c3, d3, Units:  $\text{kg/m}^2$ ). (a) is for 8:00 LST on 19 Dec., (b) is for 8:00 LST on 20 Dec., (c) is for 8:00 LST on 21 Dec., and (d) is for 8:00 LST on 22 Dec.

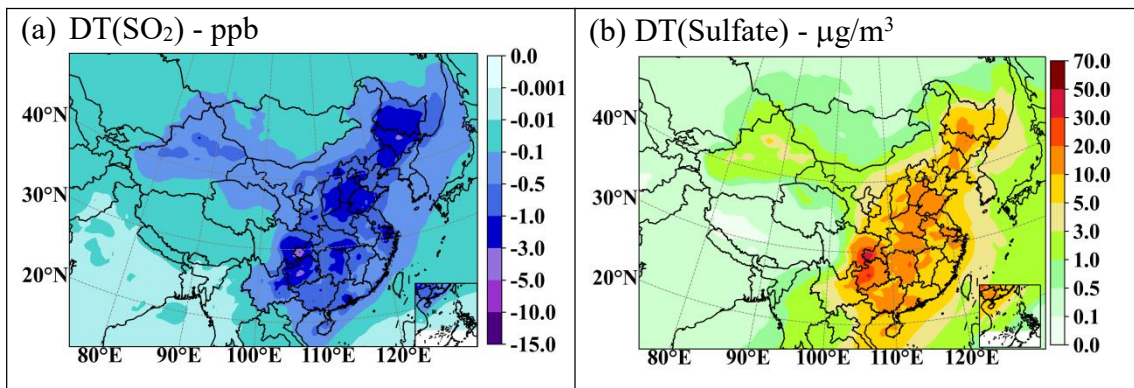


**Figure 6. The mean SO<sub>2</sub> concentration decreased (a) and sulfate concentration increased (b) by cloud chemistry for DEC.**

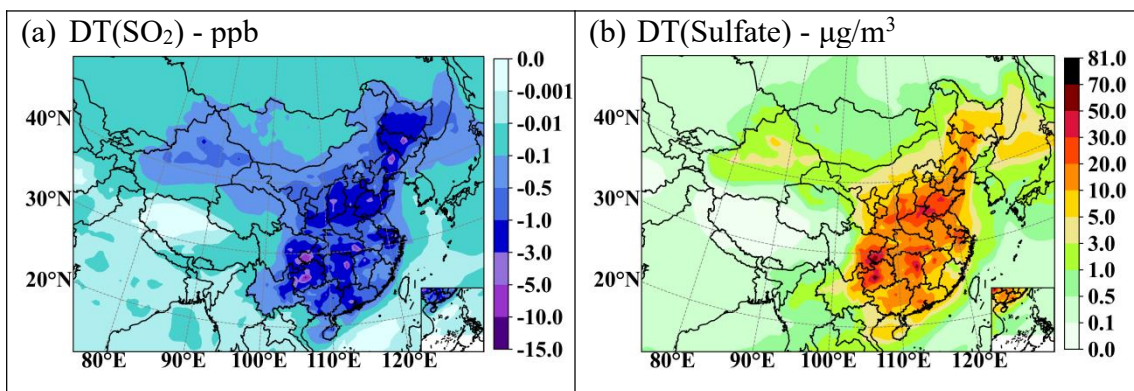


**Figure 7. The mean SO<sub>2</sub> concentration decreased (a) and sulfate concentration increased (b) by cloud chemistry for HPE-2.**



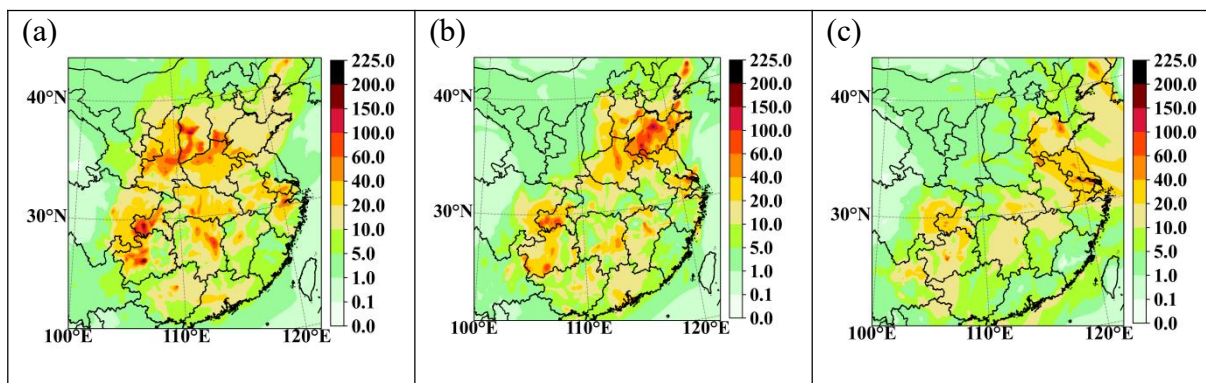


**Figure 8.** The differences in surface sulfate concentrations between with and without cloud chemistry at 21:00 on 20 Dec. (a), at 17:00 on 21 Dec. (b), and at 12:00 on 22 Dec. (c) (Units:  $\mu\text{g}/\text{m}^3$ ).

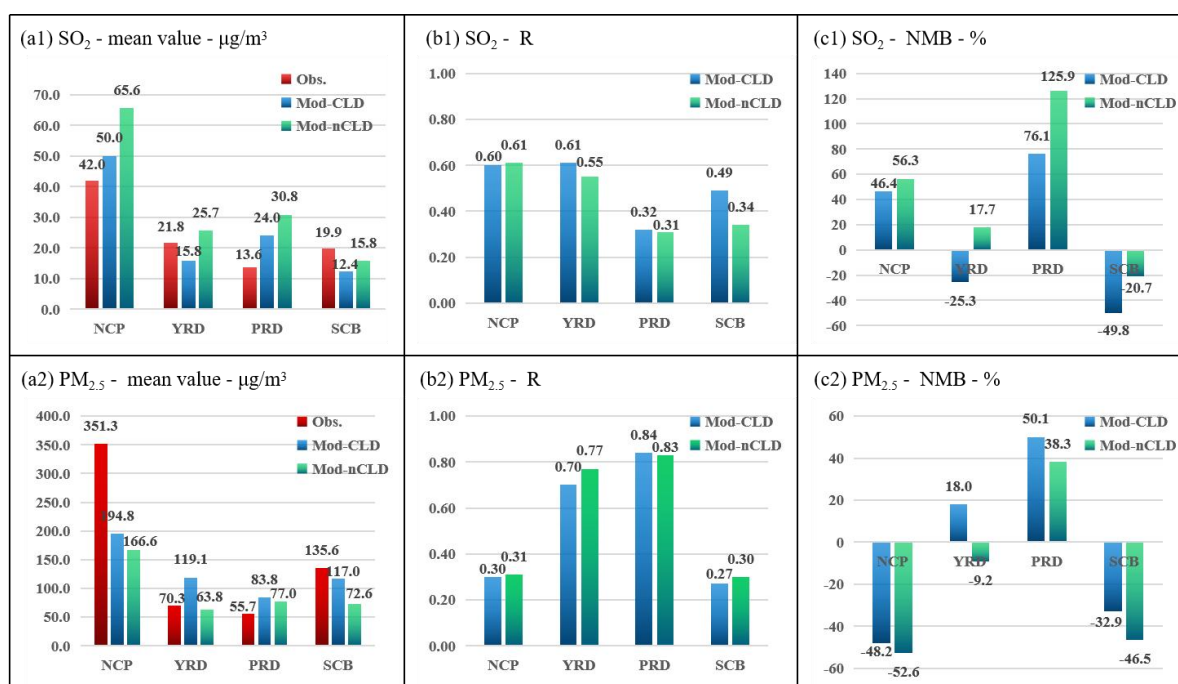


**Figure 9.** Statistical metrics for hourly  $\text{SO}_2$  and  $\text{PM}_{2.5}$  for four regions for HPE-2 with (Mod-CLD) and without (Mod-nCLD) cloud chemistry. The mean value (a1, Units:  $\mu\text{g}/\text{m}^3$ ), R (b1) and NMB (c1, Units: %) of  $\text{SO}_2$  as well as the mean value (a2, Units:  $\mu\text{g}/\text{m}^3$ ), R (b2) and NMB (c2, Units: %) of  $\text{PM}_{2.5}$ . Obs. denotes the observations.

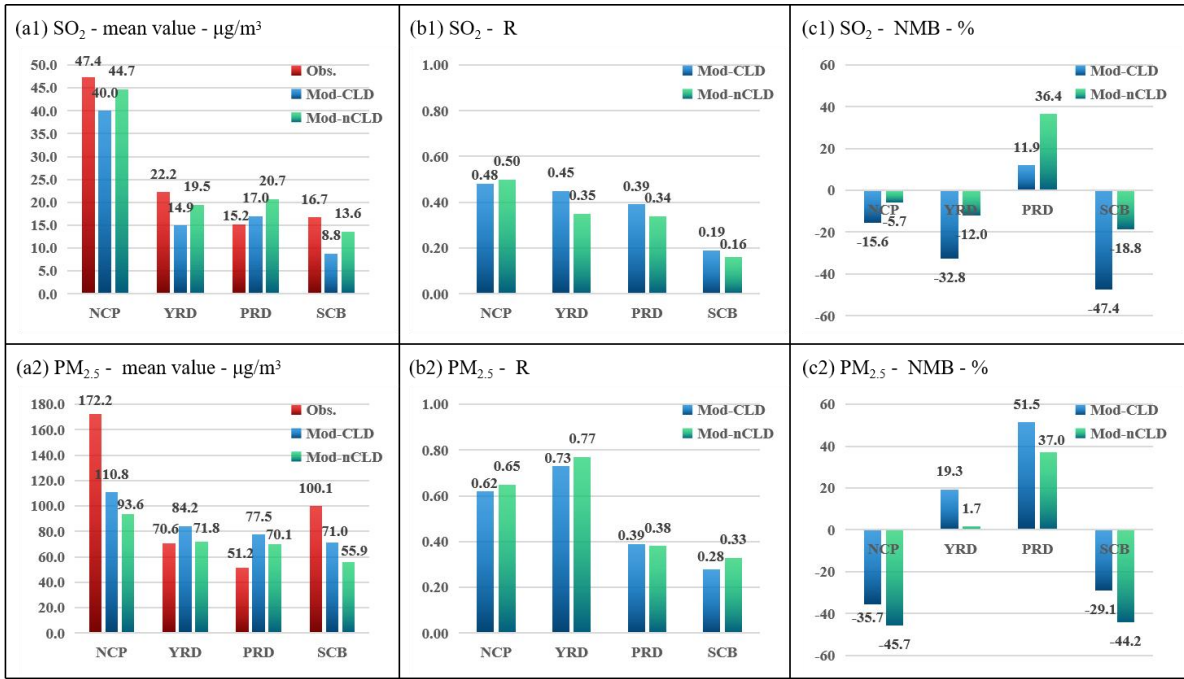


**Figure 10. Statistical metrics for hourly SO<sub>2</sub> and PM<sub>2.5</sub> for four regions for DEC with (Mod-CLD) and without (Mod-nCLD) cloud chemistry. The mean value (a1, Units: µg/m<sup>3</sup>), R (b1) and NMB (c1, Units: %) of SO<sub>2</sub> as well as the mean value (a2, Units: µg/m<sup>3</sup>), R (b2) and NMB (c2, Units: %) of PM<sub>2.5</sub>. Obs. denotes the observations.**

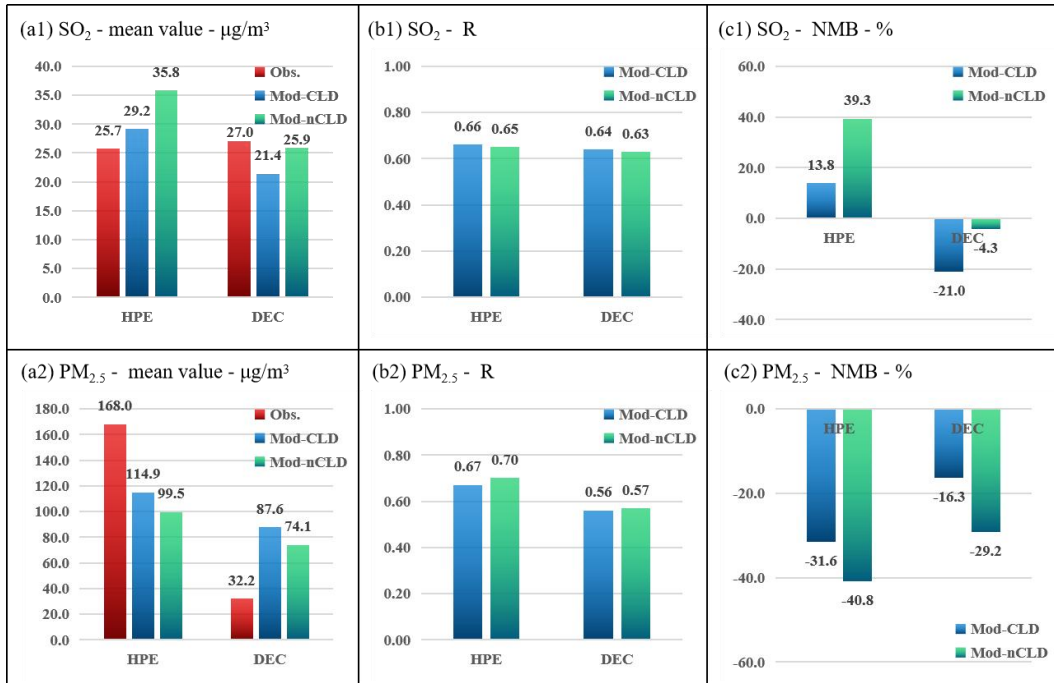


**Figure 11. Statistical metrics for hourly SO<sub>2</sub> and PM<sub>2.5</sub> in all selected sites for HPE-2 and DEC with (Mod-CLD) and without (Mod-nCLD) cloud chemistry. The mean value (a1, Units: µg/m<sup>3</sup>), R (b1) and NMB (c1, Units: %) of SO<sub>2</sub> as well as the mean value (a2, Units: µg/m<sup>3</sup>), R (b2) and NMB (c2, Units: %) of PM<sub>2.5</sub>. Obs. denotes the observations.**

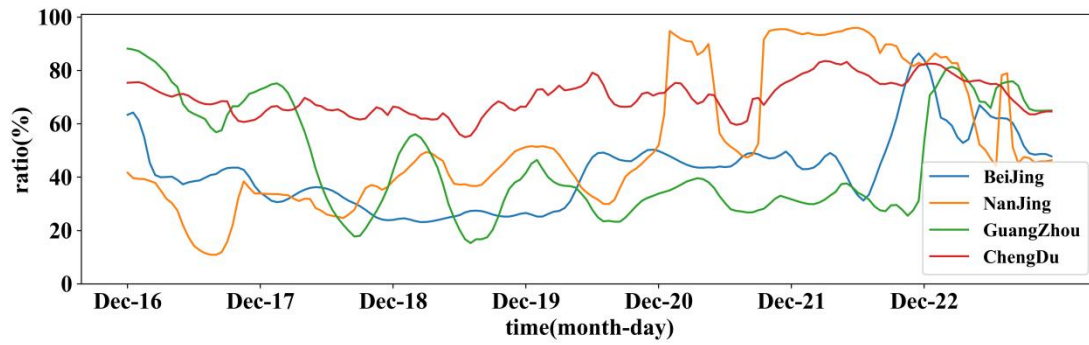


Figure 12. The rates of SO<sub>2</sub> column concentration reduced by cloud chemistry in Beijing (blue), Nanjing (yellow), Guangzhou (green) and Chengdu (red).

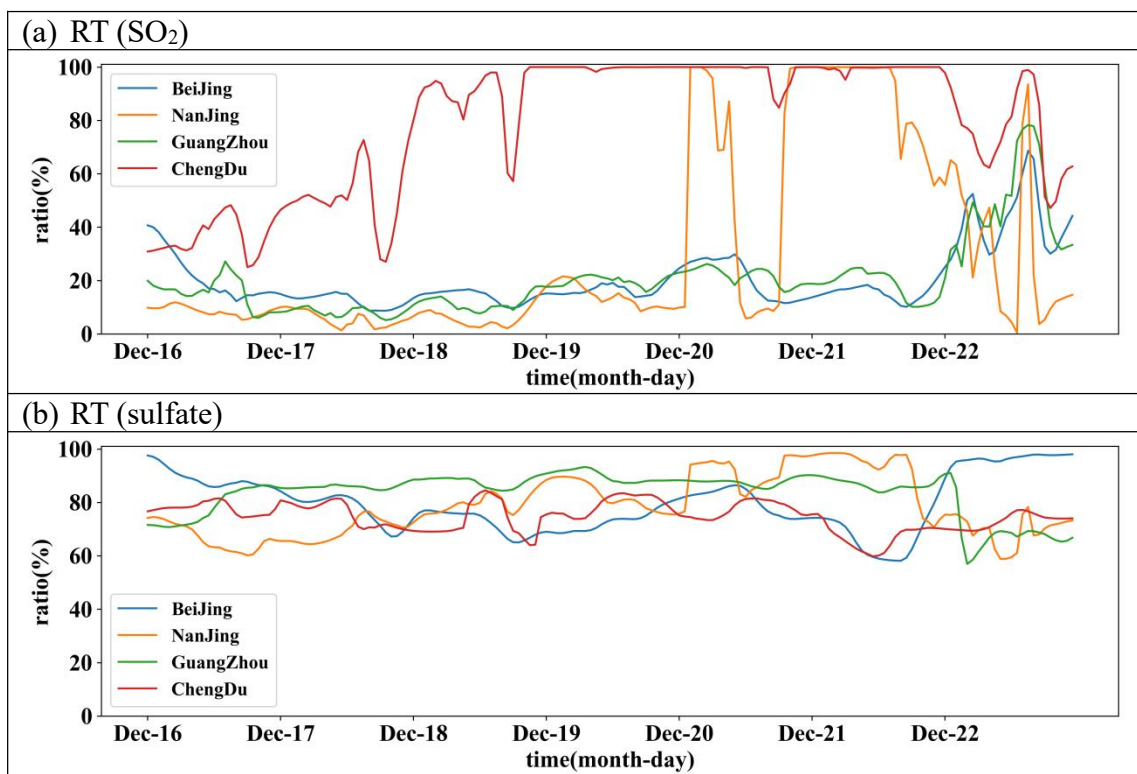
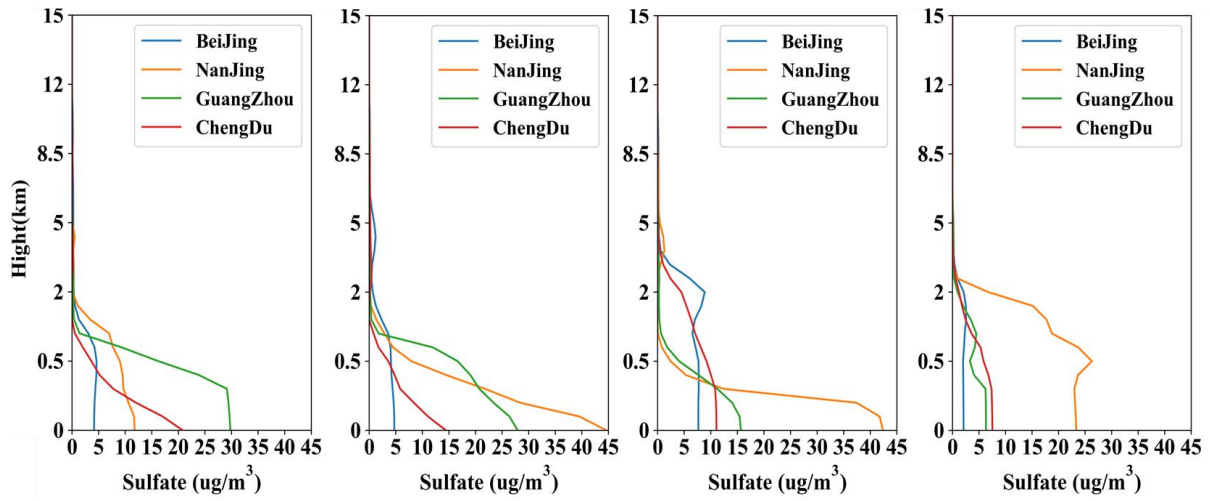


Figure 13. The rates of surface SO<sub>2</sub> reduced (a) and the surface sulfate increased (b) influenced by cloud chemistry in Beijing (blue), Nanjing (yellow), Guangzhou (green) and Chengdu (red).



**Figure 14. Vertical profiles of sulfate concentration difference (DT) at 12:00 on 20 Dec., at 21:00 on 20 Dec., at 17:00 on 21 Dec., and at 12:00 on 22 Dec. in Beijing (blue), Nanjing (yellow), Guangzhou (green) and Chengdu (red).**



**Table 1. Equilibrium Constants for the Parameterization of the Cloud Chemistry in CUACE.**

Equilibrium Relation	Constant Expression	Equilibrium Constant		
		K(298)	a	Unit
$SO_2(g) + H_2O(aq) \leftrightarrow SO_2(aq)$	$K_{HS} = \frac{[SO_2(aq)]}{[SO_2(g)]}$	1.23	3120	$\frac{M}{atm}$
$SO_2(aq) \leftrightarrow H^+ + HSO_3^-$	$K_{1S} = \frac{[H^+][HSO_3^-]}{[SO_2(aq)]}$	$1.7 \times 10^{-2}$	2090	$M$
$HSO_3^- \leftrightarrow H^+ + SO_3^{2-}$	$K_{2S} = \frac{[H^+][SO_3^{2-}]}{[HSO_3^-]}$	$6.0 \times 10^{-8}$	1120	$M$
$O_3(g) + H_2O(aq) \leftrightarrow O_3(aq)$	$K_{HO} = \frac{[O_3(aq)]}{[O_3(g)]}$	$1.15 \times 10^{-2}$	2560	$\frac{M}{atm}$
$H_2O_2(g) + H_2O(aq) \leftrightarrow H_2O_2(aq)$	$K_{HP} = \frac{[H_2O_2(aq)]}{[H_2O_2(g)]}$	$9.7 \times 10^4$	6600	$\frac{M}{atm}$

**Table 2. physics parameterization schemes in WRF.**

Physical management	Parameterization	References
microphysics scheme	Lin	Lin et al. (1983)
shortwave radiation	Goddard	Chou and Suarez (1994)
longwave radiation	RRTM	Mlawer et al. (1997)
land surface scheme	Noah	Chen and Dudhia (2001)
boundary layer scheme	MYJ	Janjić (1994)
cumulus scheme	Grell-3D	Grell (1993)

**Table 3. Statistics for SO<sub>2</sub>, O<sub>3</sub>, H<sub>2</sub>O<sub>2</sub> and sulfate in cloud chemistry at Mount Tai site.**

	Obs.	Mod	R	RAD(%)	NMB(%)	
CP-1	SO <sub>2</sub>	2.2	2.3	0.34	-3.4	7.1
	O <sub>3</sub>	97.8	55.3	0.33	27.8	-43.5
	H <sub>2</sub> O <sub>2</sub>	26.5	16.8	0.78	22.4	-36.6
	Sulfate	31.7	9.2	0.32	55.0	-71.0
CP-2	SO <sub>2</sub>	0.6	0.6	0.47	-6.1	12.9
	O <sub>3</sub>	60.7	51.0	0.40	8.7	-16.0
	H <sub>2</sub> O <sub>2</sub>	46.9	32.4	0.06	18.4	-29.6
	Sulfate	28.1	11.4	0.54	42.2	-59.4

Note: unit of SO<sub>2</sub> and O<sub>3</sub> (ppbv), H<sub>2</sub>O<sub>2</sub> (μM), and Sulfate (μg/m<sup>3</sup>)

**Table 4. Statistical metrics for meteorology in four regions for HPE and DEC**

		Obs.		Mod		R		NMB(%)		RMSE	
		HPE	DEC	HPE	DEC	HPE	DEC	HPE	DEC	HPE	DEC
N	T2	1.0	1.1	2.8	2.1	0.70	0.84	187.3	84.9	3.3	2.5
C	RH2	78.8	68.3	52.3	48.8	0.54	0.64	-33.7	-28.6	32.3	25.9
P	WS10	1.5	1.7	1.7	2.2	0.49	0.54	14.1	27.5	1.2	1.3
Y	T2	9.2	8.0	9.5	8.4	0.94	0.96	2.9	5.1	1.4	1.3
R	RH2	79.2	75.6	73.8	73.0	0.86	0.85	-6.8	-3.5	10.7	9.3
D	WS10	2.2	2.3	2.8	3.0	0.74	0.76	28.7	31.9	1.2	1.3
P	T2	18.3	17.3	19.0	17.9	0.93	0.92	3.6	3.8	1.9	1.9
R	RH2	72.2	70.4	64.3	65.4	0.76	0.68	-10.9	-7.2	14.0	13.9
D	WS10	1.8	2.4	2.0	3.2	0.67	0.72	13.6	37.1	1.0	1.5
S	T2	10.2	9.7	10.5	10.0	0.74	0.75	2.8	3.1	1.8	2.2
C	RH2	81.6	79.9	74.1	71.3	0.66	0.60	-9.2	-10.8	12.7	15.5
B	WS10	1.1	1.3	1.6	1.9	0.49	0.36	49.2	50.5	1.0	1.3

Note: unit of T2 (°C), RH2(%) and WS10 (m/s)

**Table 5. Statistical metrics for hourly SO<sub>2</sub>, O<sub>3</sub> and PM<sub>2.5</sub> in four regions for HPE and DEC**

		Obs.(µg/m <sup>3</sup> )		Mod(µg/m <sup>3</sup> )		R		NMB(%)	
		HPE	DEC	HPE	DEC	HPE	DEC	HPE	DEC
NCP	SO <sub>2</sub>	42.0	61.5	50.0	40.0	0.60	0.48	46.3	-15.6
	O <sub>3</sub>	8.8	7.4	7.4	10.9	0.47	0.60	-15.3	-32.4
	PM <sub>2.5</sub>	351.3	182.1	194.8	110.8	0.30	0.62	-48.2	-35.7
YRD	SO <sub>2</sub>	21.8	16.3	15.8	14.9	0.61	0.45	-25.3	-32.8
	O <sub>3</sub>	31.3	14.4	9.3	22.1	0.33	0.68	-54.0	-45.5
	PM <sub>2.5</sub>	70.3	82.9	119.1	84.2	0.70	0.73	18.0	19.3
PRD	SO <sub>2</sub>	13.6	24.0	24.0	17.0	0.32	0.39	76.1	11.9
	O <sub>3</sub>	45.7	56.3	56.5	57.4	0.84	0.80	23.0	13.9
	PM <sub>2.5</sub>	55.7	83.6	83.8	77.5	0.84	0.39	50.1	51.5
SCB	SO <sub>2</sub>	20.0	10.0	12.4	8.8	0.49	0.19	-49.8	-47.4
	O <sub>3</sub>	22.0	49.0	45.3	54.2	0.20	0.47	123.1	97.4
	PM <sub>2.5</sub>	135.6	91.0	117.0	71.0	0.27	0.28	-32.9	-29.1